

## **Gö-VIP-8**

**Name** Dr. rer. nat. Mei-Ling Chang Liao/ Prof. Dr. med. W.-H. Zimmermann

**Abteilung** Institut für Pharmakologie

**Titel der Publikation** Sensing Cardiac Electrical Activity with a Cardiomyocyte Targeted Optogenetic Voltage Indicator

**Publikationsorgan** Circulation Research 117:401-412 (August 2015)

**Autoren** Chang Liao ML<sup>1,3,4</sup>, de Boer TP<sup>5</sup>, Mutoh H<sup>6</sup>, Raad N<sup>2,3,7</sup>, Richter C<sup>7</sup>, Wagner E<sup>2,3</sup>, Downie BR<sup>9</sup>, Unsöld B<sup>2,10</sup>, Arooj I<sup>5</sup>, Streckfuss-Bömeke K<sup>2,3</sup>, Döker S<sup>1</sup>, Luther S<sup>3,7</sup>, Guan K<sup>2,3</sup>, Wagner S<sup>2,10</sup>, Lehnart SE<sup>2,3</sup>, Maier LS<sup>2,10</sup>, Stühmer W<sup>3,8</sup>, Wettwer E<sup>1</sup>, van Veen T<sup>5</sup>, Morlock MM<sup>4</sup>, Knöpfel T<sup>5,11,12</sup>, Zimmermann WH<sup>1,3\*</sup>

- (1) Institut für Pharmakologie, Universitätsmedizin Göttingen
- (2) Klinik für Kardiologie und Pulmonologie Germany, Universitätsmedizin Göttingen
- (3) DZHK (Deutsches Zentrum für Herz-Kreislaufforschung), Standort Göttingen
- (4) Technische Universität Hamburg-Harburg
- (5) Department of Medical Physiology, University Medical Center Utrecht
- (6) RIKEN Brain Science Institute, Saitama
- (7) Max-Planck-Institut für Dynamik und Selbstorganisation, Göttingen
- (8) Max-Planck-Institut für Experimentelle Medizin, Göttingen
- (9) Transkriptomanalyselabor, Universitätsmedizin Göttingen
- (10) Klinik für Innere Medizin II, Universitätsmedizin Regensburg
- (11) Department of Medicine and Centre for Neurotechnology, Imperial College, London

\*Corresponding Author

## **Zusammenfassung des wissenschaftlichen Inhalts**

### **(Prof. Dr. Wolfram-Hubertus Zimmermann)**

Optogenetische Werkzeuge werden für die Identifikation und Steuerung biologischer Prozesse in lebenden Zellen entwickelt. Die Beurteilung der elektrischen Aktivität des Herzens über optische Verfahren wird durch das kontinuierliche Schlagen des Herzens erschwert. Durch die stabile genetische Integration eines fluoreszierenden Spannungssensors (VSFP2.3) mit spezifischer Expression in Herzmuskelzellen sowie Anwendung von Förster-Resonanz-Energie-Transfer (FRET) Verfahren ist es nun erstmalig gelungen, die elektrische Aktivität von Herzmuskelzellen in Kultur, aber auch am frei schlagenden Herz über hochauflösende Kamerasysteme sowie optische Lichtleiter zu analysieren. Neben einer Anwendung in der Maus konnte über experimentelle Simulationen nachgewiesen werden, dass sich der von uns entwickelte Ansatz auch im Menschen anwenden lässt. Durch die spezifische Lokalisation des Spannungssensors in der Zellmembran, lassen sich darüber hinaus detaillierte Struktur-Funktionsanalysen im akuten wie chronischen Experiment durchführen. Unsere Studie zeigt damit erstmalig den Weg zur

minimal invasiven Bewertung von Herzmuskelzellentwicklung und Herzfunktion über optische Kardiogramme mittels hochauflösender Bildgebung auf.

Weitere Informationen:

Universitätsmedizin Göttingen

Institut für Pharmakologie

Prof. Dr. Wolfram-Hubertus Zimmermann

Telefon: 0551/ 39 5781

Robert-Koch-Str. 40, 37075

w.zimmermann@med.uni-goettingen.de



Mei-Ling Chang Liao Wolfram-Hubertus Zimmermann

## Genetically Encoded Voltage Indicators Mapping Cardiac Electrical Activity Under a New Light

Mario Delmar, Gregory E. Morley

Since the days of Einthoven, graphical representations of cardiac electric activity have greatly advanced our understanding of arrhythmias and their mechanisms. Throughout the 20th century, technological advances led to improvements in the temporal and spatial resolution with which electric signals were detected. Optical mapping of electric activity was made possible by the discovery of voltage sensitive dyes that report changes in light emission as a function of transmembrane potential.<sup>1</sup> A major breakthrough came with the use of high-speed cameras that can simultaneously detect the optical signal from thousands of neighboring sites, adding orders of magnitude to the spatial resolution.<sup>2</sup> As in many other fields of science, visualizing what before had only been imagined led to a rapid advance in the understanding of function. Optical mapping continues to progress and with the work of Chang Liao et al,<sup>3</sup> published in this issue of *Circulation Research*,<sup>3</sup> the field takes a new leap forward. Instead of using voltage-sensitive dyes, the authors have recorded cardiac electric activity using a genetically encoded voltage indicator (GEVI) with no apparent toxicity and a good signal/noise ratio. The data show that the emitter is a reliable reporter of activation and that it has the potential for use in minimally invasive in vivo recordings in the presence of normal blood perfusion. The results also show that the time response of the indicator is adequate to follow relatively slow events, such as the action potential morphology of human adult cardiac myocytes and human embryonic stem cell-derived cardiac myocytes. Altogether, the authors convincingly show that GEVIs can be effectively used to detect cardiac electric activity, thus adding an important new tool to the toolbox of the cardiac electrophysiologist and heralding a future of novel studies (well discussed in the article) that were not practical in the past.

---

### Article, see p 401

---

The breakthrough work of Chang Liao et al<sup>3</sup> represents an addition to, and not a replacement for, other methods. And like any new technology, it carries new limitations. Perhaps

the most important is the slow off time of the fluorophore. The authors show that the decay of signal fluorescence is best described by a single exponential with a time constant of >30 ms. This magnitude is similar to that of the entire action potential duration at 90% repolarization (APD90) of the mouse ventricle paced at a cycle length of 300 ms.<sup>4</sup> The authors do demonstrate that an empirical linear correction can adequately predict the APD90 of the cells based on the optical APD50. However, it is possible that genetic- or drug-induced changes in APD will disrupt this relation, making this new system still not the model of choice for studies where accurate determinations of APD are a priority. Furthermore, the slow kinetics of the emitter may impede an accurate spatial representation of activation waves at fast rates, such as those seen in the mouse ventricle during atrial or ventricular tachycardia. This is not to reduce the importance of the present article; only to emphasize that this new approach is a major step forward that remains complementary of others. Just like the first camera-based optical mapping study opened a huge door of investigation even if constrained by technical limitations of its time,<sup>2</sup> this study has set a major cornerstone from where to build ahead. Faster GEVIs are already being used in the neuroscience field<sup>5</sup> and are likely to be followed by others. The new approach described by Chang Liao et al<sup>3</sup> opens numerous new paths of investigation, such as the possibility of developing GEVIs that, by use of specific promoters, report from individual elements of the cardiac conduction system or even from nonmyocyte cells populating the neighborhood of surviving tissue after injury.<sup>6</sup> There is much to be known that remains veiled by technical constraints now lifted through the use of GEVIs. Exciting times are ahead, illuminated from within the genome of the cardiac cells.

### Sources of Funding

This work was supported by grants RO1-HL106632 and RO1 GM057691 (Dr Delmar) and RO1 HL076751 (Dr Morley).

### Disclosures

None.

### References

1. Salama G, Morad M. Merocyanine 540 as an optical probe of transmembrane electrical activity in the heart. *Science*. 1976;191:485-487.
2. Davidenko JM, Pertsov AV, Salomonsz R, Baxter W, Jalife J. Stationary and drifting spiral waves of excitation in isolated cardiac muscle. *Nature*. 1992;355:349-351. doi: 10.1038/355349a0.
3. Chang Liao ML, de Boer TP, Mutoh H, Raad N, Richter C, Wagner E, Downie BR, Unsöld B, Arooj I, Streckfuss-Bömeke K, Döker S, Luther S, Guan K, Wagner S, Lehnart SE, Maier LS, Stühmer W, Wettwer E, van Veen T, Morlock MM, Knöpfel T, Zimmermann WH. Sensing cardiac electrical activity with a cardiac myocyte-targeted optogenetic voltage indicator. *Circ Res*. 2015;117:401-412. doi: 10.1161/CIRCRESAHA.117.306143.

---

The opinions expressed in this article are not necessarily those of the editors or of the American Heart Association.

From The Leon H Charney Division of Cardiology, New York University School of Medicine (M.D., G.E.M.).

Correspondence to Mario Delmar, MD, PhD, The Leon H Charney Division of Cardiology, New York University School of Medicine, 522 First Ave, Smilow 805, New York, NY 10016. E-mail Mario.delmar@nyumc.org

(*Circ Res*. 2015;117:390-391.)

DOI: 10.1161/CIRCRESAHA.115.307064.)

© 2015 American Heart Association, Inc.

*Circulation Research* is available at <http://circres.ahajournals.org>

DOI: 10.1161/CIRCRESAHA.115.307064

4. Anumonwo JM, Tallini YN, Vetter FJ, Jalife J. Action potential characteristics and arrhythmogenic properties of the cardiac conduction system of the murine heart. *Circ Res.* 2001;89:329–335.
5. St-Pierre F, Marshall JD, Yang Y, Gong Y, Schnitzer MJ, Lin MZ. High-fidelity optical reporting of neuronal electrical activity with an ultra-fast fluorescent voltage sensor. *Nat Neurosci.* 2014;17:884–889. doi: 10.1038/nn.3709.
6. Vasquez C, Mohandas P, Louie KL, Benamer N, Bapat AC, Morley GE. Enhanced fibroblast-myocyte interactions in response to cardiac injury. *Circ Res.* 2010;107(8):1011–1020. doi: 10.1161/CIRCRESAHA.110.227421.

---

KEY WORDS: Editorials ■ action potentials ■ arrhythmias, cardiac ■ voltage-sensitive dye imaging

# Circulation Research

JOURNAL OF THE AMERICAN HEART ASSOCIATION



## Genetically Encoded Voltage Indicators: Mapping Cardiac Electrical Activity Under a New Light

Mario Delmar and Gregory E. Morley

*Circ Res.* 2015;117:390-391

doi: 10.1161/CIRCRESAHA.115.307064

*Circulation Research* is published by the American Heart Association, 7272 Greenville Avenue, Dallas, TX 75231

Copyright © 2015 American Heart Association, Inc. All rights reserved.

Print ISSN: 0009-7330. Online ISSN: 1524-4571

The online version of this article, along with updated information and services, is located on the  
World Wide Web at:

<http://circres.ahajournals.org/content/117/5/390>

**Permissions:** Requests for permissions to reproduce figures, tables, or portions of articles originally published in *Circulation Research* can be obtained via RightsLink, a service of the Copyright Clearance Center, not the Editorial Office. Once the online version of the published article for which permission is being requested is located, click Request Permissions in the middle column of the Web page under Services. Further information about this process is available in the [Permissions and Rights Question and Answer](#) document.

**Reprints:** Information about reprints can be found online at:  
<http://www.lww.com/reprints>

**Subscriptions:** Information about subscribing to *Circulation Research* is online at:  
<http://circres.ahajournals.org/subscriptions/>

## Sensing Cardiac Electrical Activity With a Cardiac Myocyte–Targeted Optogenetic Voltage Indicator

Mei-Ling Chang Liao, Teun P. de Boer, Hiroki Mutoh, Nour Raad, Claudia Richter, Eva Wagner, Bryan R. Downie, Bernhard Unsöld, Iqra Arooj, Katrin Streckfuss-Bömeke, Stephan Döker, Stefan Luther, Kaomei Guan, Stefan Wagner, Stephan E. Lehnart, Lars S. Maier, Walter Stühmer, Erich Wettwer, Toon van Veen, Michael M. Morlock, Thomas Knöpfel, Wolfram-Hubertus Zimmermann

**Rationale:** Monitoring and controlling cardiac myocyte activity with optogenetic tools offer exciting possibilities for fundamental and translational cardiovascular research. Genetically encoded voltage indicators may be particularly attractive for minimal invasive and repeated assessments of cardiac excitation from the cellular to the whole heart level.

**Objective:** To test the hypothesis that cardiac myocyte–targeted voltage-sensitive fluorescence protein 2.3 (VSFP2.3) can be exploited as optogenetic tool for the monitoring of electric activity in isolated cardiac myocytes and the whole heart as well as function and maturity in induced pluripotent stem cell–derived cardiac myocytes.

**Methods and Results:** We first generated mice with cardiac myocyte–restricted expression of VSFP2.3 and demonstrated distinct localization of VSFP2.3 at the t-tubulus/junctional sarcoplasmic reticulum microdomain without any signs for associated pathologies (assessed by echocardiography, RNA-sequencing, and patch clamping). Optically recorded VSFP2.3 signals correlated well with membrane voltage measured simultaneously by patch clamping. The use of VSFP2.3 for human action potential recordings was confirmed by simulation of immature and mature action potentials in murine VSFP2.3 cardiac myocytes. Optical cardiograms could be monitored in whole hearts ex vivo and minimally invasively in vivo via fiber optics at physiological heart rate (10 Hz) and under pacing-induced arrhythmia. Finally, we reprogrammed tail-tip fibroblasts from transgenic mice and used the VSFP2.3 sensor for benchmarking functional and structural maturation in induced pluripotent stem cell–derived cardiac myocytes.

**Conclusions:** We introduce a novel transgenic voltage-sensor model as a new method in cardiovascular research and provide proof of concept for its use in optogenetic sensing of physiological and pathological excitation in mature and immature cardiac myocytes in vitro and in vivo. (*Circ Res.* 2015;117:401-412. DOI: 10.1161/CIRCRESAHA.117.306143.)

**Key Words:** arrhythmias, cardiac ■ electrophysiology ■ heart ■ myocytes, cardiac ■ optical imaging ■ optogenetics ■ stem cells

Optical imaging of transmembrane voltage and intracellular calcium changes during systole and diastole offers a unique possibility to gain insight into pathophysiological processes underlying cardiac development and disease.<sup>1-3</sup> Electric recordings by extracellular (eg, surface) or impaling electrodes

Editorial, see p 390  
In This Issue, see p 389

and patch-clamp techniques are widely used for the characterization of myocardial electrophysiology from the tissue to the

Original received January 30, 2015; revision received June 9, 2015; accepted June 15, 2015. In May 2015, the average time from submission to first decision for all original research papers submitted to *Circulation Research* was 15.49 days.

From the Institute of Pharmacology (M.-L.C.L., S.D., E. Wettwer, W.-H.Z.), Clinic for Cardiology and Pulmonology (N.R., E. Wagner, B.U., K.S.-B., K.G., S.W., S.E.L., L.S.M.), and Microarray and Deep-Sequencing Facility (B.R.D.), University Medical Center Göttingen, Göttingen, Germany; DZHK (German Center for Cardiovascular Research), partner site Göttingen, Göttingen, Germany (M.-L.C.L., N.R., E. Wagner, K.S.-B., S.L., K.G., S.E.L., W.S., W.-H.Z.); Institute of Biomechanics, Technical University Hamburg-Harburg, Hamburg, Germany (M.-L.C.L., M.M.M.); Department of Medical Physiology, Division of Heart and Lungs, University Medical Center Utrecht, Utrecht, The Netherlands (T.P.d.B., I.A., T.v.V.); Laboratory of Neuronal Circuit Dynamics, RIKEN Brain Science Institute, Saitama, Japan (H.M., T.K.); Max-Planck-Institutes for Dynamics and Self Organization (N.R., C.R., S.L.) and Experimental Medicine (W.S.), Göttingen, Germany; Department of Internal Medicine II, University Hospital of Regensburg, Regensburg, Germany (B.U., S.W., L.S.M.); Department of Medicine and Centre for Neurotechnology, Imperial College London, United Kingdom (T.K.).

Current address (H.M.): Department of Neurophysiology, Hamamatsu University School of Medicine, Hamamatsu, Shizuoka, Japan.

The online-only Data Supplement is available with this article at <http://circres.ahajournals.org/lookup/suppl/doi:10.1161/CIRCRESAHA.117.306143/-DC1>.

Correspondence to Wolfram-Hubertus Zimmermann, MD, Institute of Pharmacology, Heart Research Center Göttingen, University Medical Center Göttingen, Robert-Koch-Str 40, 37075 Göttingen, Germany. E-mail [w.zimmermann@med.uni-goettingen.de](mailto:w.zimmermann@med.uni-goettingen.de)

© 2015 American Heart Association, Inc.

*Circulation Research* is available at <http://circres.ahajournals.org>

DOI: 10.1161/CIRCRESAHA.117.306143

Nonstandard Abbreviations and Acronyms	
$\alpha$ MHC	$\alpha$ -myosin heavy chain
AP	action potential
CFP	cyan fluorescent protein (Cerulean)
FRET	Förster (fluorescence) resonance energy transfer
GEVIs	genetically encoded voltage indicators
iPSCs	induced pluripotent stem cell
OCG	optical cardiograms
SR	sarcoplasmic reticulum
VSFP	voltage-sensitive fluorescent protein
YFP	yellow fluorescent protein (Citrine)

cellular level. However, classical intracellular electrophysiology is invasive, time-consuming, resource-intensive, and can typically not be performed repetitively in the same cardiac preparation over extended periods of time. Moreover, limited spatial resolution of extracellular electrophysiological techniques does not allow for precise assessment of conduction disturbances at the micrometer scale. As an alternative methodology, optical imaging of transmembrane voltage by use of voltage-sensitive dyes<sup>3-9</sup> offers higher spatial and temporal resolution, but is hampered by cardiac toxicity and the inability to

perform repeated measurements in chronic experiments. These limitations can be overcome by innovations in optogenetics, namely by the introduction of genetically encoded voltage indicators (GEVIs). Different GEVIs have been used to date mainly for imaging of electric activity in mouse<sup>10,11</sup> and *Drosophila*<sup>12</sup> brain, as well as in fish heart.<sup>13</sup> Recently, the ArcLight GEVI has been transduced in human induced pluripotent stem cell (iPSC)-derived cardiac myocytes for imaging of action potentials (APs) in drug screening applications.<sup>14</sup>

The first GEVI was reported in 1997 and consisted of a fusion between GFP and a voltage-gated ion channel.<sup>15</sup> Although this and other early GEVIs only functioned well in *Xenopus* oocytes, more recent efforts by several groups focused on the use of isolated voltage sensing domains and specifically tuned single fluorescent proteins or made use of Förster (fluorescence) resonance energy transfer (FRET).<sup>16</sup> In cardiac myocytes and especially in beating heart tissue, FRET-based ratiometric imaging is preferred as it can be applied to minimize motion artifacts.

Because of its reasonably fast kinetics, the apparent biological inertness of the voltage-sensitive domain from *Ciona intestinalis*, reliable membrane targeting in excitable tissue, and its design for ratiometric imaging, the voltage-sensitive fluorescent protein 2.3 (VSFP2.3) reporter seemed

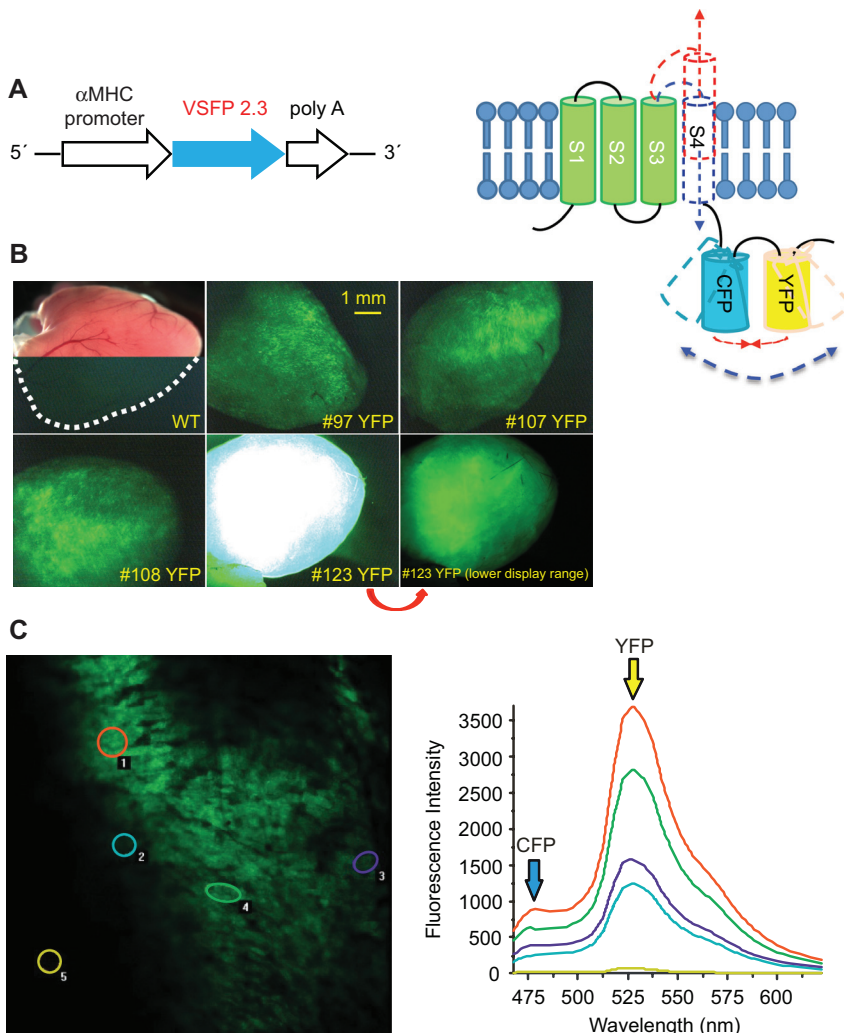


**Figure 1. Identification of transgenic mice with cardiac targeting of voltage-sensitive fluorescence protein 2.3 (VSFP2.3).** **A**, Schematic of cDNA encoding for VSFP2.3 under the control of the cardiac myocyte-restricted  $\alpha$ -myosin heavy chain ( $\alpha$ MHC) promoter and of the membrane topology as well as positional changes of the VSFP2.3 protein during cardiac depolarization and repolarization. **B**, Hearts from investigated transgenic mouse lines showed different yellow fluorescent protein (YFP) abundance; a wild-type (WT) heart analyzed with a similar camera setting is displayed for comparison; the **lower right** image corresponds to the **lower middle** image with a lower display range. **C**, Fluorescence emission spectrum from a  $\alpha$ MHC-VSFP2.3 mouse (line no. 123) heart tissue under 440 nm illumination. In the 5 color-coded regions of interest 2 emission peaks could be detected at 477 and 527 nm indicating the presence of the cyan fluorescent protein (CFP) and YFP Förster (fluorescence) resonance energy transfer pairs.

well-suited for recording membrane voltage in cardiac myocytes. To date, sensors of the VSFP family have been mainly used to report membrane voltage changes in cultured neurons as well as in the brains of living mice.<sup>10</sup> Whether VSFP2.3 would be of similar use in cardiac myocytes has not been investigated.

The purpose of this study was to establish the first cardiac optogenetic voltage sensor mouse model with robust expression and function of VSFP2.3 under the control of the cardiac myocyte-specific  $\alpha$ -myosin heavy chain ( $\alpha$ MHC) promoter.<sup>17</sup> Analysis at the cellular and whole organ level revealed no transgene toxicity and produced highly reliable optical recordings of cardiac myocyte-specific membrane voltage changes during physiologically and pathologically stimulated contraction cycles. Furthermore, we demonstrate the applicability of VSFP2.3 for the monitoring of cellular function and maturation in iPSC-derived cardiac myocytes.

## Methods

Experimental animals were maintained in accordance with the guiding principles of the American Physiological Society. Animal experiments were approved by the Niedersächsisches Landesamt für Verbraucherschutz und Lebensmittelsicherheit.

## Generation of Transgenic Mice

Transgenic mice were generated by pronuclear injection of  $\alpha$ MHC-VSFP2.3 cDNA (7783 bp; Figure 1A) released by *Bam*HI/*Pme*I digestion (Online Figure I).  $\alpha$ MHC-GCaMP2 mice were generated as reporter controls with known cardiac toxicity using a similar strategy.

## Echocardiography

Myocardial structure and function were assessed by echocardiography using a Vevo 2100 system (Visual Sonics Inc, Toronto, Canada).

## Isolation of Adult Mouse Cardiac Myocytes

Cardiac myocytes were isolated from adult transgenic mice according to a published protocol with modifications.<sup>18,19</sup>

## Immunofluorescence Staining

Adult cardiac myocytes were incubated with mouse anti-ryanodine receptor type 2 and anti-calcium channel, voltage-dependent, L-type,  $\alpha$ 1C subunit antibodies followed by suitable secondary antibodies (Online Table I) for analyses by confocal laser scanning microscopy (LSM710/NLO, Zeiss).

## RNA Sequencing and Bioinformatics

RNA sequencing was performed on an Illumina HighSeq-2000 platform (single read 50 bp; >40 Mio reads per sample). Transcripts with an average RPKM (reads per kilobase per million mapped reads) value of >1 were considered expressed and identified as differentially regulated using a minimum absolute log<sub>2</sub>-fold change of 1 and Benjamin and Hochberg-adjusted *P* value (false discovery rate) of 0.05. VSFP2.3 transcript abundance was estimated by aligning raw FASTQ RNA reads to the VSFP coding sequence using bowtie2. Gene ontology enrichment analysis of bioprocesses was performed with GOSep.<sup>20</sup> RNA sequencing data were deposited in the National Center for Biotechnology Information's Gene Expression Omnibus (GEO series accession number GSE69190).

## Combined Patch-Clamp and Fluorescence Recordings in Isolated Cardiac Myocytes

Cardiac myocytes were investigated using the patch-clamp technique under whole-cell configuration. Cyan and yellow light was detected

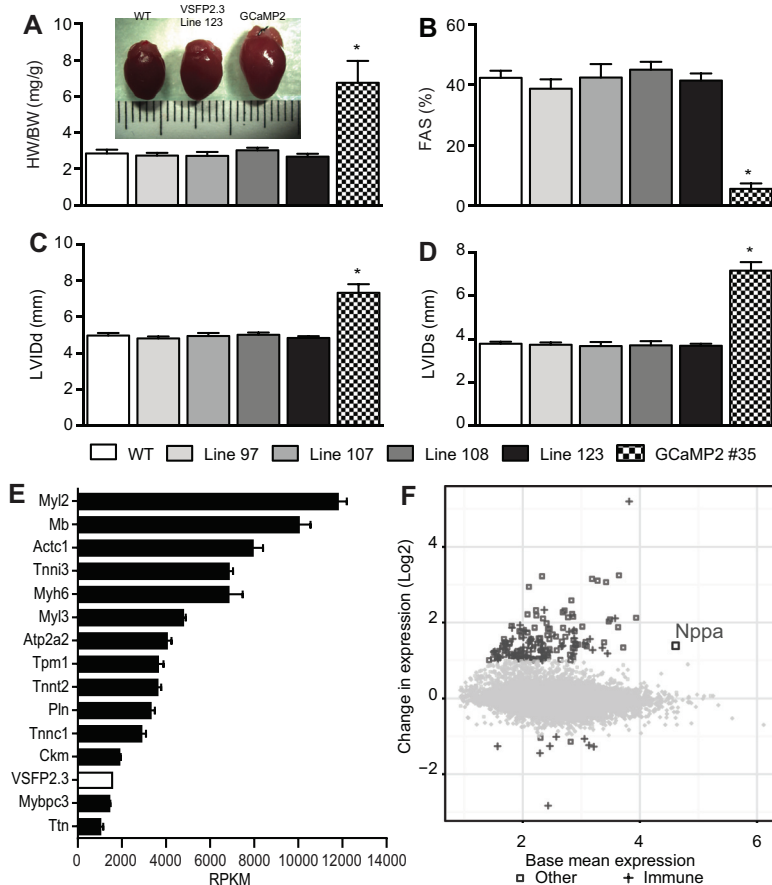


**Figure 2. Assessment of transgene toxicity in  $\alpha$ -myosin heavy chain ( $\alpha$ MHC)-voltage-sensitive fluorescence protein 2.3 (VSFP2.3) mice.**

**A**, Echocardiography at 16 weeks of age confirmed that VSFP2.3 did not cause deleterious effects: **(A)** heart weight/body weight ratio (HW/BW; HW estimated by echocardiography; inset exemplifies heart size in indicated lines), **(B)** fractional area shortening (FAS), **(C)** left ventricular dimensions in diastole (LVIDd), **(D)** left ventricular dimensions in systole (LVIDs). Note the strong pathological phenotype in  $\alpha$ MHC-GCaMP2 mice ( $n=3$  at 15 weeks of age). Wild-type (WT) and VSFP2.3 mouse lines:  $n=8$  (4/4 male/female) mice. \* $P<0.05$  vs wild-type by 1-way ANOVA with Tukey multiple comparisons test. **E**, Selection of transcripts from the 60 most abundant mRNA in WT and VSFP2.3 mice (pooled;  $n=4$ ) in direct comparison with VSFP2.3 transcript abundance in the 2 transgenic mice. **F**, Plot of all 11584 expressed protein-encoding transcripts (average reads per kilobase per million mapped reads [RPKM] >1) with the 170 differentially expressed transcripts marked either as crosses (106/170 associated with the gene ontology term immune system process) or boxes (Others). Nppa (atrial natriuretic peptide) is highlighted as the only differentially expressed cardiac gene.

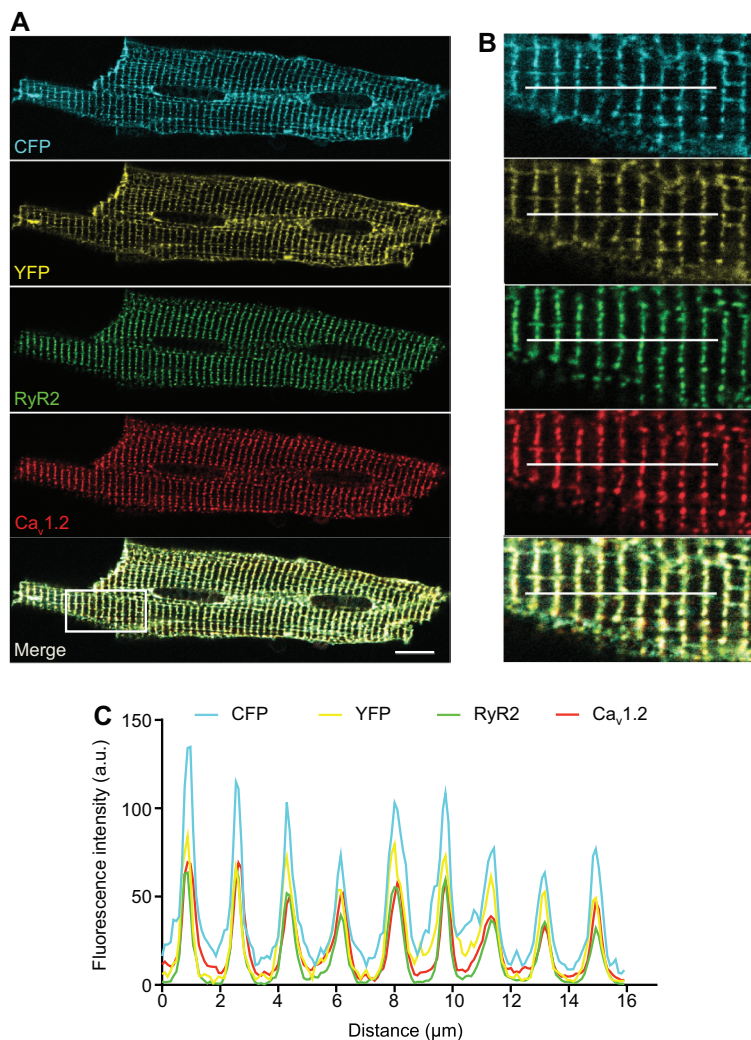


**Figure 3. Targeting of voltage-sensitive fluorescence protein 2.3 (VSFP2.3) to the t-tubulus/junctional sarcoplasmic reticulum (SR) microdomain.** **A**, Confocal microscopy in isolated adult mouse cardiac myocytes demonstrated colocalization of VSFP2.3 with the  $Ca_v1.2$   $\alpha 1$ -pore subunit of L-type calcium channels in the sarcolemma and the Ryanodine receptor type 2 (RyR2) pore-subunit at SR junctional microdomains. **B**, Enlarged from the highlighted area (white box) in the merged image in **A** with the scan-line in white used for quantification of fluorescence intensities. **C**, Fluorescence intensity plot confirming the localization of VSFP2.3 at the t-tubule/junctional SR microdomain. Scale bar, 10  $\mu$ m. CFP indicates cyan fluorescent protein; and YFP, yellow fluorescent protein.

with 2 photomultiplier tubes connected to an Optoscan system (Cairn Research; Online Figure II). Voltage-dependent fluorescence changes were assessed in voltage-clamp mode. In current-clamp experiments, APs were triggered by injecting 2 nA/2 ms currents at 1 Hz. Prerecorded APs of human embryonic stem cell-derived cardiac myocytes and human left ventricular cardiac myocytes were imposed on VSFP2.3-expressing mouse cardiac myocytes in voltage-clamp mode to assess VSFP2.3 responses to longer, simulated human APs.

### Whole Heart Optical Mapping

Hearts were imaged (MVPLAPO 0.63x, NA 0.15, Olympus) under mercury lamp (HBO103W/2, Olympus) illumination, using a  $438 \pm 24$  nm BP filter (cyan fluorescent protein [CFP] excitation, Semrock). Emitted light was band passed by a  $542 \pm 27$  nm filter (yellow fluorescent protein [YFP] emission, Semrock, Inc) and recorded with a  $100 \times 100$  pixel CMOS camera (Ultima-L, SciMedia) at a frame rate of 500 Hz.

### Fiber Optic Recordings

Three polymethyl methacrylate fibers (1 mm individual fiber diameter; Edmund Optics Inc) were assembled into a triangular array. Illumination provided by a metal halide lamp (Photofluor II, 200 W, AHF analysentechnik AG) passed a filter cube (excitation filter,  $ET436 \pm 20$  nm; excitation dichroic, 455 nm LF) and was guided through the optic fiber bundle to directly illuminate the heart. Emission light was collected by the same fiber bundle, passed through a second (emission) filter cube (emission dichroic, 510 nm

LPXR; CFP,  $ET480 \pm 40$  nm; YFP,  $ET535 \pm 30$  nm), and directed to 2 EMCCD cameras (Cascade 128+, Photometrics) for separate recordings of CFP and YFP signals. Proof-of-concept experiments were performed first in Langendorff-perfused hearts and subsequently in anesthetized (2% isoflurane) and mechanically ventilated mice via a left lateral thoracotomy.

### Generation of $\alpha$ MHC-VSFP2.3/Neomycin Resistance Gene iPSC Lines

iPSCs were generated from tail tip fibroblasts of a double transgenic mouse-expressing VSFP2.3 and a neomycin resistance gene under the control of the cardiac myocyte-restricted  $\alpha$ MHC promoter (Online Figure III) according to standard protocols.<sup>21</sup> The genotype was confirmed by polymerase chain reaction and evidence for pluripotency was collected by reverse transcriptase polymerase chain reaction and immunofluorescent staining for stemness markers (Online Table I).

### Differentiation and Selection of Cardiac Myocytes From $\alpha$ MHC-VSFP2.3/Neomycin Resistance Gene iPSCs

Cardiac differentiation was performed in spinner flasks for 11 days followed by additional 7 days of G418 (200  $\mu$ g/mL) for cardiac myocyte selection. Resulting embryoid bodies showed spontaneous beating and were subsequently dissociated enzymatically. Purity of cardiac myocytes was assessed by flow cytometry (BD LSR III) after staining for sarcomeric  $\alpha$ -actinin (Sigma). iPSC-derived cardiac

myocytes were cultured as monolayers for additional 5 or 12 days. For FRET imaging, iPSC-derived cardiac myocytes were plated on custom-made recording chambers, paced at 1 Hz under field stimulation and recorded with a dual photomultiplier setup (IonOptix) with appropriate CFP and YFP filters (CFP excitation,  $436 \pm 20$  nm; emission,  $480 \pm 40$  nm [CFP] and  $535 \pm 30$  nm [YFP]).

### Statistics

Data are displayed as mean  $\pm$  SEM unless stated otherwise. AP kinetics were calculated by a custom-made algorithm programmed in Matlab. Fluorescence signals were low-pass filtered at 250 Hz before determining AP characteristics. Statistical analyses were performed using Prism5 software (GraphPad) and the respectively indicated tests. The probability of a type I error was set to  $\alpha=0.05$ .

Detailed Methods are available in the Online Data Supplement.

## Results

### Stable Expression of VSFP2.3 With No Evidence for Cardiotoxicity

Forty-three pups were obtained from  $\approx 200$  pronuclear injections, and 6 transgenic founder candidates were selected by genotyping. Offspring from 4 of 6 founders ( $F_0$ -generation) showed unambiguous myocardial YFP fluorescence, indicating VSFP2.3 expression throughout the heart, with differences in expression strength in the individual  $\alpha$ MHC-VSFP2.3 founders (Figure 1B). Fluorescence emission spectrum scans demonstrated the anticipated spectral properties of VSFP2.3 with characteristic peaks at 477 nm (Cerulean/CFP) and 527

nm (Citrine/YFP), confirming expression of both fluorescent proteins (Figure 1C).

Based on previous reports and our own experience, overexpression of optogenetic transgenes in the heart (such as GCaMP2<sup>22</sup>) can impair cardiac function or myocardial structure. We tested for potential transgene toxicity by echocardiography in male and female transgenic mice ( $n=4$ /sex/mouse line) and did not find differences in myocardial structure and contractility in the  $\alpha$ MHC-VSFP2.3 lines and control wild-type mice (Figure 2A–2D; Online Figure IV), confirming that the VSFP2.3 did not cause cardiotoxicity even at high abundance (line no. 123); this was in marked contrast to mice overexpressing the GCaMP2 calcium sensor under  $\alpha$ MHC control. We further scrutinized VSFP2.3 transcript abundance and whether transcription of protein encoding genes was altered by VSFP2.3 overexpression. VSFP2.3 was among the 60 most abundant transcripts identified by RNA sequencing, expressed at similar level as myosin-binding protein C (Mybpc3) and  $\approx 4$ -fold lower as compared with  $\alpha$ MHC (Myh6; Figure 2E). Only 170 of the expressed 11 584 protein encoding transcripts were identified as differentially regulated in VSFP2.3 mice (Figure 2F), with 106 of those associated with the gene ontology term immune system process. Nppa (atrial natriuretic peptide) was the only differentially expressed cardiac gene, suggesting a mild molecular, but structurally and functionally unapparent phenotype. This

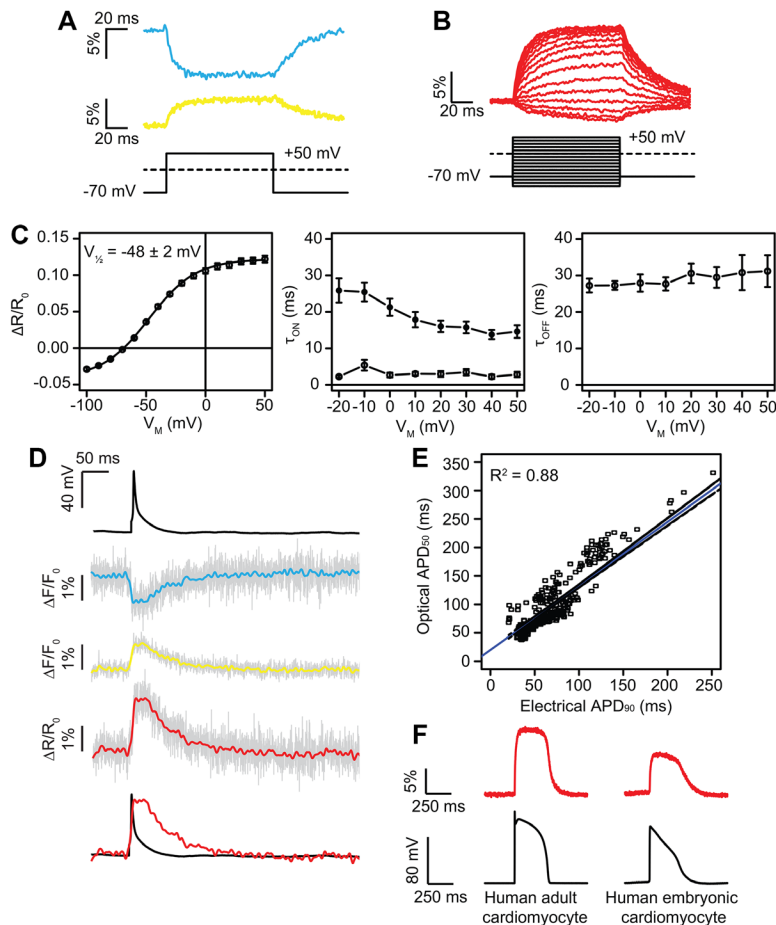


**Figure 4. Determination of voltage–fluorescence relationship.**

**A**, Representative traces of patch-clamp experiment in a cardiac myocyte from a  $\alpha$ -myosin heavy chain ( $\alpha$ MHC)-voltage-sensitive fluorescence protein 2.3 (VSFP2.3) mouse according to the depicted voltage clamp protocol with the anticipated decrease in cyan fluorescent protein (CFP) and Förster (fluorescence) resonance energy transfer (FRET)-induced increase in yellow fluorescent protein (YFP) fluorescence. **B**, FRET signals (YFP/CFP ratios, red traces) at indicated holding potentials (black traces). **C**, Steady-state FRET ratio as a function of defined membrane potentials and on/off kinetics of the VSFP2.3 reporter ( $n=10$ ). **D**, Stimulated action potentials (APs) with corresponding CFP, YFP, and FRET signals; superimposed electric and optical AP for direct comparison of the respective kinetics. **E**, Linear correlation with confidence interval between optical APD<sub>50</sub> and electric APD<sub>50</sub> (action potential duration at 50 and 90% repolarization) (358 APs from 7 cardiac myocytes analyzed). **F**, Simulated human adult and embryonic cardiac myocyte APs with the AP clamp technique in  $\alpha$ MHC-VSFP2.3 mouse (line no. 123) cardiac myocytes.

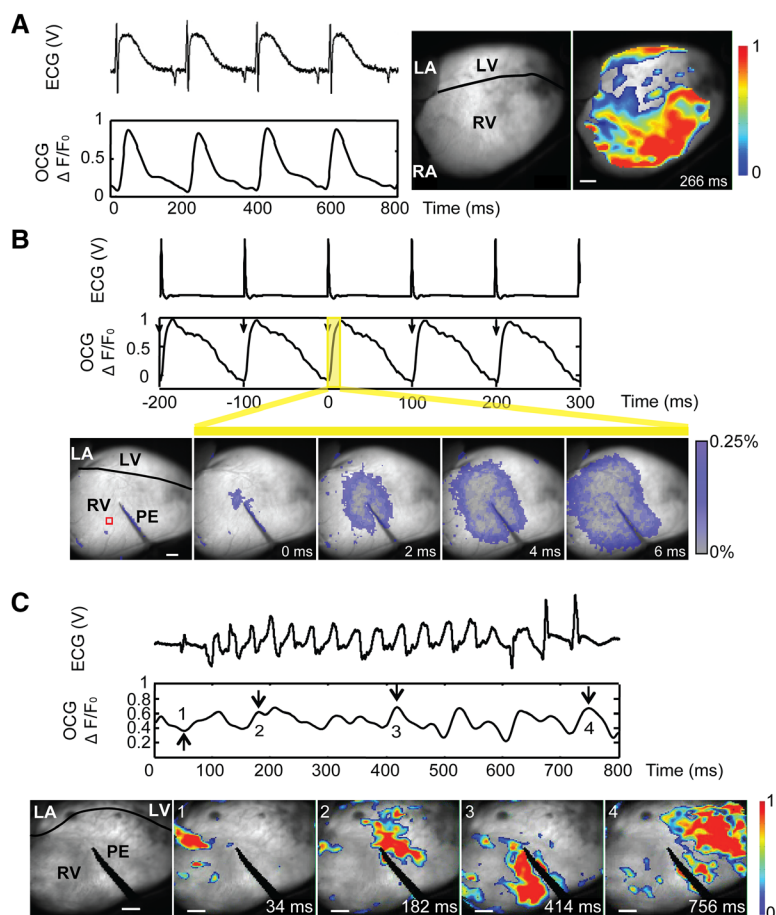


**Figure 5. Optical mapping of action potential (AP) propagation in Langendorff-perfused hearts.** **A**, Synchronous ECG and optical cardiogram (OCG) recordings (yellow fluorescent protein [YFP] emission under cyan fluorescent protein [CFP] excitation) from a Langendorff-perfused  $\alpha$ -myosin heavy chain-voltage-sensitive fluorescence protein 2.3 (no. 123) heart during sinus rhythm (screen shot from Online Movie I at the indicated time point). **B**, ECG and OCG traces during 10 Hz electric pacing via a point electrode (PE; visible above the epicardial surface of the right ventricle [RV]). Black arrows indicate the initiation of the electric pulses. Yellow OCG signal area delineates single frames visualizing anisotropic excitation spread below. Red box in left picture: region of interest used for OCG recording (screen shots from Online Movie II at the indicated time points). **C**, ECG and OCG traces during a ventricular arrhythmia. Recordings were performed after termination of a 12.5-Hz 200-pulse train for arrhythmia induction. Numbered arrows correspond to single frame images below (screen shots from Online Movie III at the indicated time points). Scale bars, 1 mm. LA indicates left atrium; LV, left ventricle; and RA, right atrium.

lack of transgene toxicity was further confirmed by patch clamping of cardiac myocytes from WT and VSFP2.3#123 mice (Online Table II).

### Targeting of VSFP2.3 to the t-Tubulus/Junctional SR Microdomain

Confocal microscopy of isolated cardiac myocytes suggested that VSFP2.3 was strictly localized to sarcolemmal membranes and the abundant transverse (t)-tubule membrane invaginations typical for mature cardiac myocytes (Figure 3A). Costaining for the sarcolemmal  $Ca_v1.2$ ,  $\alpha1C$  pore-subunit and the principal intracellular SR calcium release channel in the heart, that is, the ryanodine receptor type 2, confirmed the anticipated localization of VSFP2.3 at the t-tubulus/junctional SR microdomain (Figure 3B and 3C). Interestingly, VSFP2.3 was also highly expressed at the cell surface, both at the intercalated disc and the lateral surface membrane.

### VSFP2.3 Reports Membrane Voltage in Cardiac Myocytes

Isolated adult cardiac myocytes subjected to voltage steps under whole-cell patch-clamp configuration showed voltage-dependent fluorescence changes similar to the properties of VSFP2.3 measured in PC12 cells and cortical neurons,<sup>23,24</sup> with decreased CFP fluorescence and increased YFP fluorescence on membrane depolarization (Figure 4A). The baseline normalized ratio of YFP over CFP fluorescence ( $\Delta R/R_0$ ;

Figure 4B) was measured during the last 10 ms of each 100 ms voltage step and could be well fitted with a Boltzmann function, revealing a half maximal optical response at  $-48 \pm 2$  mV ( $n=10$ ) and a dynamic range of 15%  $\Delta R/R_0$  (Figure 4C, left).

To assess the kinetics of VSFP2.3 in cardiac myocytes, we fitted the rising and falling fluorescence intensities in response to voltage steps with a single or double exponential function and found that the rising signals were best described by 2 time constants,  $\tau_{ON,fast}$  and  $\tau_{ON,slow}$  of  $3 \pm 0.8$  and  $16 \pm 1.6$  ms, respectively (Figure 4C, middle;  $n=10$ , at +20 mV). Fluorescence signal decay was well fitted by a single exponential function with a time constant  $\tau_{OFF} = 31 \pm 3$  ms (Figure 4C, right;  $n=10$ , at +20 mV).

The relatively slow on time constant accounted for the lack of the phenotypically characteristic fast phase 0 depolarization of mouse cardiac myocyte APs in VSFP2.3 responses (Figure 4D). Despite the slow off time constant of VSFP2.3, we observed that electric and optical APD (action potential duration) correlated well, with the strongest correlation noted between electric  $APD_{90}$  and optical  $APD_{50}$  ( $R^2=0.88$ ;  $P<2.2e-16$ ), suggesting that bona fide electric repolarization ( $APD_{90}$ ) can be approximated robustly from the optical  $APD_{50}$  values in mouse cardiac myocytes (Figure 4E) by linear regression analysis: electric  $APD_{90} = 1.125 \times \text{optical } APD_{50} + 19.8$  ms. Stimulation with the adrenergic receptor agonist isoprenaline (1  $\mu\text{mol/L}$ ) and increasing electric stimulation

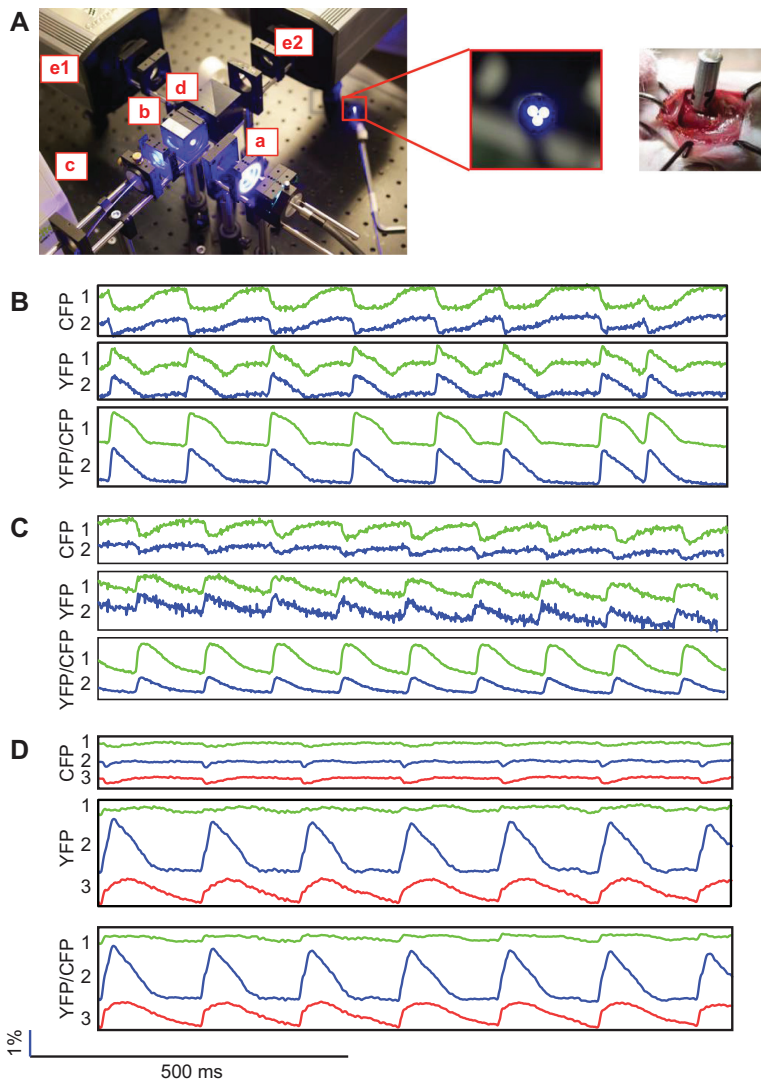


**Figure 6. Optical cardiogram recordings using fiber optics.** **A**, Optical fiber setup (left). (a) light source, (b) excitation filter cube, (c) optic fiber bundle, (d) emission filter cube, (e1, e2) cascade cameras for the recordings of cyan fluorescent protein (CFP) and yellow fluorescent protein (YFP) signals, respectively. The enlarged image shows the tip of the fiber bundle (3× polymethyl methacrylate fiber 1 mm) (right). The fiber bundle placed against a beating heart in situ. Representative CFP, YFP recordings, and optical action potential traces during spontaneous beating in vitro without (**B**) and with (**C**) the addition of blebbistatin (used to suppress motion artifacts). **D**, In vivo recordings of membrane voltage using fiber optics. Note: Signals from only 2 channels are displayed in **B** and **C**.

frequency (0.5–2 Hz) shortened the optical APD as anticipated (Online Figure V). Simulations of the longer lasting human APs from adult cardiac myocytes and the slower APs from human embryonic stem cell–derived cardiac myocytes in VSFP2.3-mouse cardiac myocytes with the AP clamp technique indicated the applicability of the VSFP2.3 sensor for evaluations of upstroke and repolarization in human cardiac myocytes (Figure 4F).

### Optical Cardiogram Recordings in VSFP2.3 Transgenic Mouse Hearts

For assessing whether cardiac myocyte-restricted VSFP2.3 could be exploited to record optical cardiograms (OCGs), a fast camera system at a frame rate of 500 Hz was used to visualize the endogenous YFP signal response from the epicardium (8×8 mm field of view) under CFP excitation. Fractional changes of YFP signals ( $\Delta F/F$ ) were derived and denoted as optical APs or OCGs. As the maximum fractional change using this imaging configuration did not exceed 2.5%, spatiotemporal filtering with binning of 3×3 or 5×5 pixels was performed to increase the signal/noise ratio of the OCG. At sinus rhythm, OCGs were synchronous

with the simultaneously recorded ECGs (Figure 5A; Online Movie I). Importantly, electric pacing of the heart at the physiological frequency of 10 Hz confirmed 1:1 capture, evidenced by robust OCG signal spread (Figure 5B; Online Movie II). Subsequently, activation times were selected using a 50% threshold and signal averaging from consecutive pacing cycles was used to construct representative activation maps from the cardiac VSFP2.3 signal. These data confirmed that the transgenic VSFP2.3 sensor captures the expected anisotropic activation spread in the heart at maximal conduction velocity of  $0.58 \pm 0.14$  m/s and minor perpendicular conduction velocity of  $0.25 \pm 0.08$  m/s ( $n=6$ ). Finally, we resolved fast, abnormal cardiac rhythms classified by anatomic origin as ventricular arrhythmia induced by 200-pulse trains administered at 12.5 Hz (Figure 5C; Online Movie III).

### Development of a Fiber Optic System for In Vivo OCG Recordings

To advance toward our goal of minimally invasive in vivo recordings of spread of excitation, we assembled a prototype fiber optic imaging system for ratiometric analysis of VSFP2.3

signals, comprising a bundle of 3 optical fibers connected to 2 high-speed cameras (Figure 6A). We first tested this set-up in Langendorff-perfused, spontaneously beating hearts from  $\alpha$ MHC-VSFP2.3 mice (line no. 123) without (Figure 6B) and with (Figure 6C) the application of blebbistatin (used for electromechanical uncoupling) and observed the anticipated CFP/YFP signals in both groups. Proof-of-concept *in vivo* studies confirmed the use of the fiber optic approach in the presence of normal blood perfusion (Figure 6D), with signal kinetics similar to the ones observed in the Langendorff experiments (Table).

### VSFP2.3 in iPSC-Derived Cardiac Myocytes for Functional and Morphological Studies

Finally, we tested the use of the VSFP2.3 sensor in documenting structural and functional maturation in iPSC-derived cardiac myocytes. For this, we first generated double transgenic mice by crossing  $\alpha$ MHC-neomycin resistance gene (expression of the neomycin resistance in cardiac myocytes<sup>25</sup>) and  $\alpha$ MHC-VSFP2.3 mice (line no. 123; Online Figure IIIA). iPSC lines were then generated from tail tip fibroblast using standard procedures and pluripotency was confirmed (Online Figure IIIB and IIIC). Under G418 selection in spinner flask cultures, cardiac myocyte purities of >85% could be achieved (Figure 7A). In extended cardiac myocyte cultures, that is, 11+7+5 and 11+7+12 days, clear sarcolemma targeting of VSFP2.3 was visible (Figure 7B). However, the lack of t-tubulation at both investigated time points confirmed low structural maturity in iPSC-derived cardiac myocytes (refer to Figure 3 for comparison with the classical signal pattern in an adult cardiac myocyte from a  $\alpha$ MHC-VSFP2.3 mouse [line no. 123]). Despite limited structural maturation, we could exploit the VSFP2.3 expression to study membrane voltage changes in iPSC-derived cardiac myocytes (Figure 7C). The fractional change in

CFP/YFP-FRET ( $\Delta R/R$ ) in iPSC-derived cardiac myocytes was  $\approx 4\%$  (Figure 7D) and thus comparable with the signals observed in adult cardiac myocytes (Table). Notably, signal increase velocity (max. upstroke,  $5.3 \pm 0.6$  versus  $2.8 \pm 0.1$   $\Delta R/s$ ) and signal duration ( $APD_{90}$ ,  $209 \pm 22$  versus  $491 \pm 46$ ) clearly distinguished adult from fetal-like iPSC-derived cardiac myocytes (Table). Importantly, simultaneous recordings of electric  $APD_{90}$  and optical  $APD_{50}$  correlated similarly well in iPSC-derived cardiac myocytes (Online Figure VI) as in adult cardiac myocytes (Figure 4E) from VSFP2.3 mice; note however that electrophysiological recordings in the small iPSC-derived cardiac myocytes was technically difficult to perform.

### Discussion

Optogenetic tools are evolving rapidly and have been widely introduced to monitor and control neuronal activity.<sup>23,26</sup> With the introduction of channelrhodopsin-2 into cardiac myocytes it became possible to control the beating behavior in isolated cardiac myocyte and whole heart preparations.<sup>27</sup> For monitoring of electric activity in whole heart, chemical probes remain the gold-standard since their introduction  $\approx 40$  years ago.<sup>8</sup> Here, we demonstrate the use of an advanced GEVI and classical targeted transgenesis to introduce VSFP2.3 into cardiac myocytes for *in vitro* and *in vivo* monitoring of physiological and pathological electric activity in mature and immature cardiac myocytes as well as whole hearts. In addition, we provide proof of concept for the use of VSFP2.3 in benchmarking cardiac myocyte maturation.

Advantages of GEVIs when compared with classical low molecular weight voltage-sensitive dyes include (1) homogeneous signal intensity independent of organ perfusion and cellular uptake, (2) cell-specific targeting of GEVIs, and (3) the applicability in longitudinal studies with repeated

**Table. Summary of VSFP2.3 Parameters**

	Whole Heart						
	In Vitro		In Vivo	Adult CMs			iPSC-CMs
	Optical Mapping	Fiber Optics	Fiber Optics	VSFP	Current Clamp*	Adult CMs	
Max. $\Delta R/R$ , %	$1.8 \pm 0.2 \dagger$	$1.1 \pm 0.1$	1.2	$2 \pm 0.2$	$102 \pm 6$	$4.96 \pm 0.48$	$3.95 \pm 0.28$
Max. upstroke, $s^{-1}$	$2.7 \pm 0.4 \dagger$	$2 \pm 0.2$	1.5	$5.5 \pm 0.3$	$201 \pm 43$	$5.3 \pm 0.6$	$2.8 \pm 0.1$
$APD_{20}$ , ms	N.D.	$29 \pm 3$	43	$71 \pm 23$	$2.6 \pm 0.5$	$89 \pm 13$	$171 \pm 9$
$APD_{50}$ , ms	$60 \pm 9$	$50 \pm 3$	65	$100 \pm 26$	$13 \pm 17$	$142 \pm 16$	$251 \pm 23$
$APD_{90}$ , ms	$87 \pm 8$	$79 \pm 6$	111	$181 \pm 35$	$71 \pm 21$	$209 \pm 22$	$491 \pm 46$
Temperature, °C	37	37	37	37	37	RT	RT
Beating frequency (bpm)	600 (point stimulation)	$505 \pm 31$ (sinus rhythm)	364 (sinus rhythm)	60 (point stimulation)	60 (field stimulated)	60 (field stimulated)	60 (field stimulated)
n	6	4	2	7	4	4	3

VSFP2.3 signals were recorded in whole heart or CM with stable expression of VSFP2.3 (all from  $\alpha$ -myosin heavy chain-VSFP2.3 no. 123).  $APD_{20/50/90}$  indicates action potential duration at 20, 50, and 90% repolarization; bpm, beats per minute; CFP, cyan fluorescent protein (Cerulean); CM, cardiac myocyte; iPSC, induced pluripotent stem cell; RT, room temperature; VSFP2.3, voltage-sensitive fluorescence protein 2.3; and YFP, yellow fluorescent protein (Citrine).

\*Data recorded by parallel patch clamping (current clamp mode) in adult cardiac myocytes are displayed for comparison (max.  $\Delta R/R$  is in millivolt and upstroke velocity is in volt per second). Data are displayed as mean  $\pm$  SEM.

Values are based on the evaluation of the CFP/YFP Förster (fluorescence) resonance energy transfer ratio ( $\Delta R/R$ ) with the exception of the optical mapping experiment ( $\dagger \Delta F/F$  YFP under CFP excitation).

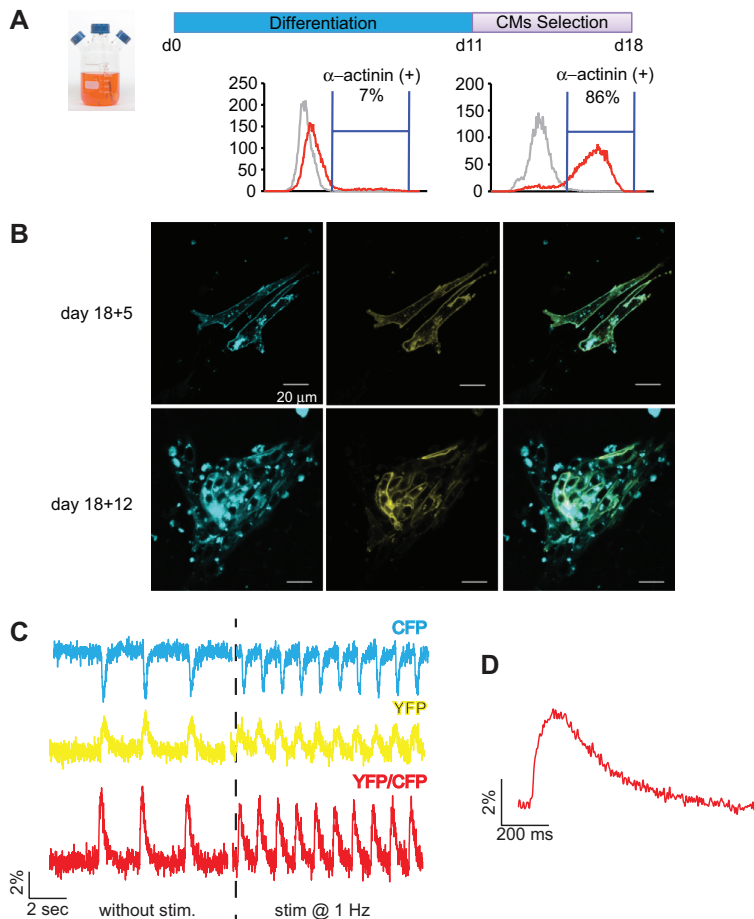


**Figure 7. Assessment of morphology and function in induced pluripotent stem cell (iPSC)-derived cardiac myocytes from  $\alpha$ -myosin heavy chain-voltage-sensitive fluorescence protein 2.3/neoR double transgenic mice.** **A**, iPSCs were differentiated in bioreactor cultures for 11 days followed by selection in the presence of G418 for additional 7 days; unselected cell pools contained <10% and selected cell pools >85% cardiac myocytes (flow cytometry was performed on culture days 11 and 18, respectively). **B**, Selected iPSC-derived cardiac myocytes were plated as monolayer cultures and subjected to live cell confocal microscopy after 5 and 12 additional days in culture; clear membrane localization of the sensor was visible. Scale bars, 20  $\mu$ m. **C**, Optical imaging of cyan fluorescent protein (CFP) and yellow fluorescent protein (YFP) and corresponding YFP/CFP-Förster (fluorescence) resonance energy transfer ratio ( $\Delta R/R$ ) in iPSC-cardiac myocyte without and under 1 Hz field stimulation on culture day 11+7+1. **D**, Average of 10 optical action potentials (under electric stimulation at 1 Hz).

measurements in the same tissue sample. For studies in cardiac myocytes, FRET-based GEVIs seem advantageous, because of the possibilities to (1) correct for intensity changes as a consequence of out-of-plane motion during contraction, which typically requires electromechanical uncoupling by pharmacological means (eg, 2,3-butanedione monoxime [BDM]<sup>28</sup> or blebbistatin<sup>29</sup>) and (2) calibrate the ratiometric FRET value for better quantitative comparison of individual experimental results in tissues and cells.

Caveats of transgenic reporters in the heart include unwanted effects on myocardial structure and function. Depending on the mouse model and strain as well as transgene abundance, even the commonly used fluorescent proteins such as GFP can elicit cardiotoxic effects.<sup>30</sup> Another example is the inadvertent developmental cardiac toxicity associated with the GCaMP2 calcium reporter, making it necessary to limit its expression to defined postnatal time windows.<sup>22</sup> Conversely, VSFP2.3 seemed to be biologically inert and did not cause any notable functional or structural changes, allowing us to study the mouse model with the highest VSFP2.3 expression and thus the strongest signal ( $\alpha$ MHC-VSFP-line no. 123). Molecular evidence by RNA sequencing confirmed no dysregulation of cardiac structural and ion channel genes, but suggested an otherwise unapparent immune response, potentially elicited by the transgenic expression of nonmammalian peptides (ie, voltage-sensitive domain of *C intestinalis*, CFP, and YFP).

FRET-based sensors typically show <10%  $\Delta R/R$ . Therefore, they require dedicated and low-noise detection systems for proper signal recording and processing. VSFP2.3 showed high maximal  $\Delta R/R$  (>10% in voltage clamp analyses) with an appropriate dynamic range for monitoring the physiological cardiac myocyte voltage range ( $-80$  to  $+20$  mV; Figure 4C). The on and off kinetics of VSFP2.3 are, however, not fast enough to faithfully report the fastest components of the cardiac myocyte AP and the nonlinear fluorescence-voltage relationship saturates at the peak of the AP. Collectively, this resulted in an apparent plateau and a prolonged duration ( $APD_{90}$ , 180–200 ms) of the optical membrane potential recorded in isolated adult mouse cardiac myocytes (Figure 4D). Optical recordings using the voltage-sensitive aminonaphthylpyridium dye di-4-ANEPPS,<sup>31</sup> impaling electrode measurements,<sup>32</sup> and monophasic AP recordings<sup>33</sup> revealed  $APD_{90}$  values of 30 to 65 ms in mouse ventricular myocardium. Thus, VSFP2.3 cannot replace the state-of-the-art electrophysiological recordings in studies where the shape of the AP is in the center of interest. However, it is important to note that despite these limitations, we found a strong correlation of the VSFP2.3  $APD_{50}$  and patch-clamp recorded  $APD_{90}$  (Figure 4E), suggesting that using mathematical models,<sup>34</sup> the electric AP could be inferred from the optical membrane potential. Moreover, the VSFP2.3 sensor was well suited to study the spread of electric excitation in whole heart preparations ex vivo (Figure 5) and in vivo (Figure 6); the latter is currently not possible with

chemical probes. Although not directly demonstrated in this study, performing series of in vivo optical measurements will be possible in  $\alpha$ MHC-VSFP2.3 mice or cross-breeds with additional genetic modifications. Finally, introducing voltage transients derived from human cardiac myocyte APs in VSFP2.3 mouse cardiac myocytes provided conceptual evidence for the suitability of cardiac myocyte-targeted VSFP2.3 in monitoring cardiac myocyte APs in species with intrinsically slower repolarization ( $APD_{90}$ ,  $\approx 300$  ms in human versus  $<100$  ms in mouse).<sup>35–38</sup>

Targeting of VSFP2.3 to the sarcolemma is essential for its voltage-dependent activity and may even allow for the analysis of sarcolemma-associated subcompartments such as t-tubules by super-resolution microscopy<sup>39</sup> using biophysically optimized fluorochromes (ie, with enhanced stability under high-power laser excitation and reduction in physical size). A particularly exciting application could be the parallel optical assessment of membrane voltage changes and calcium release events at the sarcolemma/SR dyads. Robust labeling of the t-tubular system in adult mouse cardiac myocytes with the VSFP sensor suggests that in principle this would be possible if multi-color super-resolution imaging becomes accessible.

In addition to functional imaging, the use of VSFP to benchmark cardiac myocyte growth and maturation seems to be an attractive methodology. Fetal up to early postnatal cardiac myocytes lack any or have only a residual t-tubular membrane system.<sup>40–42</sup> Accordingly, we observed no t-tubulation in iPSC-derived cardiac myocytes even in extended (30 days) monolayer cultures. In line with the resetting of somatic cells to a fetal state, iPSC-derived cardiac myocytes could be also clearly distinguished from adult cardiac myocytes by their slower optical AP upstroke and slower repolarization (Table). Although we cannot provide evidence for enhanced maturation under the conditions studied, our experimental data support the notion that longitudinal studies can be performed minimal invasively in the same cell preparation for screening of to date unknown maturation factors. Similarly and as suggested by others, GEVIs can be used in drug screens for arrhythmogenic potential.<sup>14,43</sup> In contrast to studies using voltage indicator dyes, GEVIs would also allow studies on chronic exposure to drugs or other stimuli.

A key objective of our study was to introduce VSFP2.3 for imaging of cardiac electric activity or OCG in vivo. Presently, voltage-sensitive dyes (eg, di-4-ANEPPS) are typically used in ex vivo Langendorff-perfused hearts in combination with excitation–contraction uncouplers (eg, blebbistatin or BDM) to study epicardial spread of electric activation. This strategy cannot be applied in vivo because of the toxicity of the commonly used dyes and the incompatibility of the in vivo use of electromechanical uncouplers as well as their effects on AP morphology.<sup>6,44–47</sup> Here, we provide first experimental evidence that a GEVI, expressed stably and homogeneously in cardiac myocyte membranes in vivo, can overcome these limitations. We first scrutinized the VSFP-imaging modality in Langendorff-perfused hearts and validated its use for the visualization of myocardial electric conduction under physiological and pathological heart

rate and rhythm (Figure 5). For minimally invasive in vivo recordings, we developed a fiber optic system and collected evidence for its applicability also in the absence of electromechanical uncouplers (Figure 6). In proof-of-concept studies in vivo, we could finally demonstrate its applicability in blood-perfused hearts (Figure 6D). Importantly, AP values recorded ex vivo (Tyrode's perfused) and in vivo (blood perfused) at physiological heart rates were similar (Table). With further advances of the imaging technology (ie, smaller optical fibers and multiple-fiber arrays; optimized positioning of the fiber array on the epicardial surface), we anticipate that spatial resolution can be further improved. In addition, further advanced GEVIs (eg, with near-infrared reporters) may ultimately also allow for closed chest imaging of heart rate and rhythm with to date unsurpassed spatial and temporal resolution.

Taken together, our study established first proof of concept for the use of a genetically targeted FRET-based GEVI for the visualization of electric activity in isolated cardiac myocytes of different developmental stages and the whole heart and in vivo, with and without electromechanical uncouplers. We anticipate that further optimized GEVIs<sup>11</sup> and the application of novel fluorochromes for deep tissue imaging and super-resolution imaging together with advanced engineering of optical detection systems will advance the field to enable reliable membrane voltage recordings (OCGs) in chronic experiments, with applications in studies of fundamental cardiovascular biology and drug screens, in addition to more specific applications such as monitoring of electromechanical coupling of cell grafts for heart regeneration.

## Acknowledgments

We thank Dr S. Verheule (Maastricht) for the introduction into optical imaging and Y. Iwamoto, B. Knocke, U. Leonhardt, R. Blume, and M. Zoremba for excellent technical assistance.

## Sources of Funding

We acknowledge financial support from the DZHK (German Center for Cardiovascular Research; W.H. Zimmermann and S.E. Lehnart), the German Research Foundation (DFG ZI 708/7-1, 8-1, 10-1 [W.H. Zimmermann], SFB 1002 TP A03 [L.S. Maier], A04 [K. Guan], A05/B05 [S.E. Lehnart], C03 [S. Luther] and C04/S [W.H. Zimmermann], SFB 937 A18 [S. Luther, W.H. Zimmermann]), the German Federal Ministry for Science and Education (BMBF FKZ 13GW0007A [CIRM] to W.H. Zimmermann), the European Union FP7 CARE-MI (W.H. Zimmermann) and EUTrigTreat (S.E. Lehnart), the National Institutes of Health (U01 HL099997 to W.H. Zimmermann), and RIKEN (H. Mutoh and T. Knöpfel). T.P. de Boer is supported by a Netherlands Heart Foundation fellowship (2010T45).

## Disclosures

None.

## References

- Herron TJ, Lee P, Jalife J. Optical imaging of voltage and calcium in cardiac cells & tissues. *Circ Res*. 2012;110:609–623. doi: 10.1161/CIRCRESAHA.111.247494.
- Crocini C, Coppini R, Ferrantini C, Pavone FS, Sacconi L. Functional cardiac imaging by random access microscopy. *Front Physiol*. 2014;5:403. doi: 10.3389/fphys.2014.00403.

3. Yan P, Acker CD, Zhou WL, Lee P, Bollensdorff C, Negrean A, Lotti J, Sacconi L, Antic SD, Kohl P, Mansvelder HD, Pavone FS, Loew LM. Palette of fluorinated voltage-sensitive hemicyanine dyes. *Proc Natl Acad Sci USA*. 2012;109:20443–20448. doi: 10.1073/pnas.1214850109.
4. Fluhler E, Burnham VG, Loew LM. Spectra, membrane binding, and potentiometric responses of new charge shift probes. *Biochemistry*. 1985;24:5749–5755.
5. Lang D, Sulkin M, Lou Q, Efimov IR. Optical mapping of action potentials and calcium transients in the mouse heart. *J Vis Exp*. 2011;55:3275. doi: 10.3791/3275. <http://www.jove.com/details.php?id=3275>.
6. Cheng Y, Mowrey KA, Nikolski V, Tchou PJ, Efimov IR. Mechanisms of shock-induced arrhythmogenesis during acute global ischemia. *Am J Physiol Heart Circ Physiol*. 2002;282:H2141–H2151. doi: 10.1152/ajpheart.00561.2001.
7. Salama G, Choi BR. Images of Action Potential Propagation in Heart. *News Physiol Sci*. 2000;15:33–41.
8. Salama G, Morad M. Merocyanine 540 as an optical probe of transmembrane electrical activity in the heart. *Science*. 1976;191:485–487.
9. Matiukas A, Mitrea BG, Qin M, Pertsov AM, Shvedko AG, Warren MD, Zaitsev AV, Wuskell JP, Wei MD, Watras J, Loew LM. Near-infrared voltage-sensitive fluorescent dyes optimized for optical mapping in blood-perfused myocardium. *Heart Rhythm*. 2007;4:1441–1451. doi: 10.1016/j.hrthm.2007.07.012.
10. Akemann W, Mutoh H, Perron A, Rossier J, Knöpfel T. Imaging brain electric signals with genetically targeted voltage-sensitive fluorescent proteins. *Nat Methods*. 2010;7:643–649. doi: 10.1038/nmeth.1479.
11. Akemann W, Mutoh H, Perron A, Park YK, Iwamoto Y, Knöpfel T. Imaging neural circuit dynamics with a voltage-sensitive fluorescent protein. *J Neurophysiol*. 2012;108:2323–2337. doi: 10.1152/jn.00452.2012.
12. Cao G, Platasa J, Pieribone VA, Raccuglia D, Kunst M, Nitabach MN. Genetically targeted optical electrophysiology in intact neural circuits. *Cell*. 2013;154:904–913. doi: 10.1016/j.cell.2013.07.027.
13. Tsutsui H, Higashijima S, Miyawaki A, Okamura Y. Visualizing voltage dynamics in zebrafish heart. *J Physiol*. 2010;588:2017–2021. doi: 10.1113/jphysiol.2010.189126.
14. Leyton-Mange JS, Mills RW, Macri VS, Jang MY, Butte FN, Ellinor PT, Milan DJ. Rapid cellular phenotyping of human pluripotent stem cell-derived cardiomyocytes using a genetically encoded fluorescent voltage sensor. *Stem Cell Reports*. 2014;2:163–170. doi: 10.1016/j.stemcr.2014.01.003.
15. Siegel MS, Isacoff EY. A genetically encoded optical probe of membrane voltage. *Neuron*. 1997;19:735–741.
16. Sakai R, Repunte-Canonigo V, Raj CD, Knöpfel T. Design and characterization of a DNA-encoded, voltage-sensitive fluorescent protein. *Eur J Neurosci*. 2001;13:2314–2318.
17. Subramaniam A, Jones WK, Gulick J, Wert S, Neumann J, Robbins J. Tissue-specific regulation of the alpha-myosin heavy chain gene promoter in transgenic mice. *J Biol Chem*. 1991;266:24613–24620.
18. Kabaeva Z, Zhao M, Michele DE. Blebbistatin extends culture life of adult mouse cardiac myocytes and allows efficient and stable transgene expression. *Am J Physiol Heart Circ Physiol*. 2008;294:H1667–H1674. doi: 10.1152/ajpheart.01144.2007.
19. O'Connell TD, Rodrigo MC, Simpson PC. Isolation and culture of adult mouse cardiac myocytes. *Methods Mol Biol*. 2007;357:271–296. doi: 10.1385/1-59745-214-9:271.
20. Young MD, Wakefield MJ, Smyth GK, Oshlack A. Gene ontology analysis for RNA-seq: accounting for selection bias. *Genome Biol*. 2010;11:R14. doi: 10.1186/gb-2010-11-2-r14.
21. Somers A, Jean JC, Sommer CA, et al. Generation of transgene-free lung disease-specific human induced pluripotent stem cells using a single excisable lentiviral stem cell cassette. *Stem Cells*. 2010;28:1728–1740. doi: 10.1002/stem.495.
22. Tallini YN, Ohkura M, Choi BR, et al. Imaging cellular signals in the heart in vivo: Cardiac expression of the high-signal Ca<sup>2+</sup> indicator GCaMP2. *Proc Natl Acad Sci USA*. 2006;103:4753–4758. doi: 10.1073/pnas.0509378103.
23. Mutoh H, Perron A, Akemann W, Iwamoto Y, Knöpfel T. Optogenetic monitoring of membrane potentials. *Exp Physiol*. 2011;96:13–18. doi: 10.1113/expphysiol.2010.053942.
24. Perron A, Mutoh H, Akemann W, Gautam SG, Dimitrov D, Iwamoto Y, Knöpfel T. Second and third generation voltage-sensitive fluorescent proteins for monitoring membrane potential. *Front Mol Neurosci*. 2009;2:5. doi: 10.3389/neuro.02.005.2009.
25. Klug MG, Soonpaa MH, Koh GY, Field LJ. Genetically selected cardiomyocytes from differentiating embryonic stem cells form stable intracardiac grafts. *J Clin Invest*. 1996;98:216–224. doi: 10.1172/JCI118769.
26. Williams SC, Deisseroth K. Optogenetics. *Proc Natl Acad Sci USA*. 2013;110:16287. doi: 10.1073/pnas.1317033110.
27. Brueggemann T, Malan D, Hesse M, Beiert T, Fuegemann CJ, Fleischmann BK, Sasse P. Optogenetic control of heart muscle in vitro and in vivo. *Nat Methods*. 2010;7:897–900. doi: 10.1038/nmeth.1512.
28. Kettlewell S, Walker NL, Cobbe SM, Burton FL, Smith GL. The electrophysiological and mechanical effects of 2,3-butane-dione monoxime and cytochalasin-D in the Langendorff perfused rabbit heart. *Exp Physiol*. 2004;89:163–172. doi: 10.1113/expphysiol.2003.026732.
29. Brack KE, Narang R, Winter J, Ng GA. The mechanical uncoupler blebbistatin is associated with significant electrophysiological effects in the isolated rabbit heart. *Exp Physiol*. 2013;98:1009–1027. doi: 10.1113/expphysiol.2012.069369.
30. Huang WY, Aramburu J, Douglas PS, Izumo S. Transgenic expression of green fluorescence protein can cause dilated cardiomyopathy. *Nat Med*. 2000;6:482–483. doi: 10.1038/74914.
31. Baker LC, London B, Choi BR, Koren G, Salama G. Enhanced dispersion of repolarization and refractoriness in transgenic mouse hearts promotes reentrant ventricular tachycardia. *Circ Res*. 2000;86:396–407.
32. Anumonwo JM, Tallini YN, Vetter FJ, Jalife J. Action potential characteristics and arrhythmogenic properties of the cardiac conduction system of the murine heart. *Circ Res*. 2001;89:329–335.
33. Knollmann BC, Schober T, Petersen AO, Sirenko SG, Franz MR. Action potential characterization in intact mouse heart: steady-state cycle length dependence and electrical restitution. *Am J Physiol Heart Circ Physiol*. 2007;292:H614–H621. doi: 10.1152/ajpheart.01085.2005.
34. Akemann W, Lundby A, Mutoh H, Knöpfel T. Effect of voltage sensitive fluorescent proteins on neuronal excitability. *Biophys J*. 2009;96:3959–3976. doi: 10.1016/j.bpj.2009.02.046.
35. Mummery C, Ward D, van den Brink CE, Bird SD, Doevendans PA, Ophoff T, Brutel de la Riviere A, Tertoolen L, van der Heyden M, Pera M. Cardiomyocyte differentiation of mouse and human embryonic stem cells. *J Anat*. 2002;200:233–242.
36. Zhang J, Wilson GF, Soerens AG, Koonce CH, Yu J, Palecek SP, Thomson JA, Kamp TJ. Functional cardiomyocytes derived from human induced pluripotent stem cells. *Circ Res*. 2009;104:e30–e41. doi: 10.1161/CIRCRESAHA.108.192237.
37. Kuzmenkin A, Liang H, Xu G, Pfannkuche K, Eichhorn H, Fatima A, Luo H, Saric T, Wernig M, Jaenisch R, Hescheler J. Functional characterization of cardiomyocytes derived from murine induced pluripotent stem cells in vitro. *FASEB J*. 2009;23:4168–4180. doi: 10.1096/fj.08-128546.
38. Blazeski A, Zhu R, Hunter DW, Weinberg SH, Boheler KR, Zambidis ET, Tung L. Electrophysiological and contractile function of cardiomyocytes derived from human embryonic stem cells. *Prog Biophys Mol Biol*. 2012;110:178–195. doi: 10.1016/j.pbiomolbio.2012.07.012.
39. Wagner E, Lauterbach MA, Kohl T, et al. Stimulated emission depletion live-cell super-resolution imaging shows proliferative remodeling of T-tubule membrane structures after myocardial infarction. *Circ Res*. 2012;111:402–414. doi: 10.1161/CIRCRESAHA.112.274530.
40. Lieu DK, Liu J, Siu CW, McNeerney GP, Tse HF, Abu-Khalil A, Huser T, Li RA. Absence of transverse tubules contributes to non-uniform Ca<sup>2+</sup> wavefronts in mouse and human embryonic stem cell-derived cardiomyocytes. *Stem Cells Dev*. 2009;18:1493–1500. doi: 10.1089/scd.2009.0052.
41. Robertson C, Tran DD, George SC. Concise review: maturation phases of human pluripotent stem cell-derived cardiomyocytes. *Stem Cells*. 2013;31:829–837. doi: 10.1002/stem.1331.
42. Itzhaki I, Schiller J, Beyar R, Satin J, Gepstein L. Calcium handling in embryonic stem cell-derived cardiac myocytes: of mice and men. *Ann NY Acad Sci*. 2006;1080:207–215. doi: 10.1196/annals.1380.017.
43. Jonsson MK, Vos MA, Mirams GR, Duker G, Sartipy P, de Boer TP, van Veen TA. Application of human stem cell-derived cardiomyocytes in safety pharmacology requires caution beyond hERG. *J Mol Cell Cardiol*. 2012;52:998–1008. doi: 10.1016/j.yjmcc.2012.02.002.
44. Cheng Y, Li L, Nikolski V, Wallick DW, Efimov IR. Shock-induced arrhythmogenesis is enhanced by 2,3-butanedione monoxime compared

- with cytochalasin D. *Am J Physiol Heart Circ Physiol*. 2004;286:H310–H318. doi: 10.1152/ajpheart.00092.2003.
45. Hayashi H, Miyauchi Y, Chou CC, Karagueuzian HS, Chen PS, Lin SF. Effects of cytochalasin D on electrical restitution and the dynamics of ventricular fibrillation in isolated rabbit heart. *J Cardiovasc Electrophysiol*. 2003;14:1077–1084.
46. Brines L, Such-Miquel L, Gallego D, Trapero I, Del Canto I, Zarzoso M, Soler C, Pelechano F, Cánoves J, Alberola A, Such L, Chorro FJ. Modifications of mechanoelectric feedback induced by 2,3-butanedione monoxime and Blebbistatin in Langendorff-perfused rabbit hearts. *Acta Physiol (Oxf)*. 2012;206:29–41. doi: 10.1111/j.1748-1716.2012.02441.x.
47. Swift LM, Asfour H, Posnack NG, Arutunyan A, Kay MW, Sarvazyan N. Properties of blebbistatin for cardiac optical mapping and other imaging applications. *Pflugers Arch*. 2012;464:503–512. doi: 10.1007/s00424-012-1147-2.

## Novelty and Significance

### What Is Known?

- Voltage-sensitive dyes are used widely for optical imaging of electric activity *ex vivo*, but not *in vivo*.
- Optogenetic tools enable optical monitoring and control of cellular activity *in vitro* and *in vivo*.

### What New Information Does This Article Contribute?

- Introduction of the first mouse model with cardiac myocyte–restricted expression of voltage-sensitive fluorescence protein 2.3 (VSFP2.3), a genetically encoded voltage indicator.
- Demonstration of robust membrane voltage imaging in cardiac myocytes *ex vivo* (isolated adult cardiac myocytes), *in situ* (Langendorff-perfused heart), *in vivo* (open chest fiber optics), and *in vitro* (induced pluripotent stem cell–derived cardiac myocytes) without cardiac toxicity.
- Transgenic VSFP2.3 enabled benchmarking of structural (t-tubulation) and functional (optical cardiograms) properties in isolated embryonic and adult cardiac myocytes and whole hearts.

Optogenetic tools are evolving rapidly for monitoring and controlling cellular activity. VSFP2.3 is particularly attractive for studying structural and functional properties of cardiac myocytes and

whole hearts, because of its targeted expression at the sarcolemma and ratiometric fluorescence energy transfer recordings to minimize motion artifacts in beating hearts. Lack of apparent toxicity is another important prerequisite, especially for longitudinal studies *in vivo* and *in vitro* cardiac myocyte cultures. The demonstration that human action potentials can also be visualized by VSFP2.3 documents its use beyond rodent models. Importantly, optical cardiograms could be used to map electric impulse propagation with high temporal and spatial resolution in Langendorff-perfused hearts. *In situ* fiber optic recordings in spontaneously beating blood-perfused hearts provided proof of concept for the applicability of VSFP2.3 in minimal invasive assessments of impulse propagation *in vivo*. Collectively, the results of this study provide evidence for the versatile use of VSFP2.3 in assessments of cardiac myocyte structure and function. We anticipate that genetically encoded voltage indicators such as VSFP2.3 will find broad applications in fundamental studies of cardiac myocyte and heart development, assessments of structural and functional alterations in heart disease, and scrutiny of innovative therapeutics, including the assessment of electric integration of cardiac myocyte grafts in attempts to remuscularize failing hearts.

## Sensing Cardiac Electrical Activity with a Cardiomyocyte Targeted Optogenetic Voltage Indicator

Mei-Ling Chang Liao<sup>1,3,4</sup>, Teun de Boer<sup>5</sup>, Hiroki Mutoh<sup>6</sup>, , Nour Raad<sup>2,3,7</sup>, Claudia Richter<sup>7</sup>, Eva Wagner<sup>2,3</sup>, Bryan R. Downie<sup>9</sup>, Bernhard Unsöld<sup>2,10</sup>, Iqra Arooj<sup>5</sup>, Katrin Streckfuss-Bömeke<sup>2,3</sup>, Stephan Doeker<sup>1</sup>, Stefan Luther<sup>3,7</sup>, Kaomei Guan<sup>2,3</sup>, Stefan Wagner<sup>2,10</sup>, Stephan Lehnart<sup>2,3</sup>, Lars S. Maier<sup>2,10</sup>, Walter Stühmer<sup>3,8</sup>, Erich Wettwer<sup>1</sup>, Toon van Veen<sup>5</sup>, Michael M. Morlock<sup>4</sup>, Thomas Knöpfel<sup>5,11,12</sup>, Wolfram-Hubertus Zimmermann<sup>1,3</sup>

Institute of Pharmacology<sup>1</sup> and Clinic for Cardiology and Pulmonology<sup>2</sup>, Heart Research Center Göttingen, University Medical Center Göttingen, Germany; DZHK (German Center for Cardiovascular Research), partner site Göttingen<sup>3</sup>; Technical University Hamburg-Harburg, Hamburg, Germany<sup>4</sup>; Department of Medical Physiology, Division of Heart & Lungs, University Medical Center Utrecht, The Netherlands<sup>5</sup>; RIKEN Brain Science Institute, Saitama, Japan<sup>6</sup>; Max-Planck-Institutes for Dynamic and Self Organization<sup>7</sup> and Experimental Medicine<sup>8</sup>, Göttingen, Germany; Microarray and Deep-Sequencing Facility, University Medical Center Göttingen, Germany<sup>9</sup>; Department of Internal Medicine II, University Hospital of Regensburg, Germany<sup>10</sup>; Department of Medicine<sup>11</sup> and Centre for Neurotechnology<sup>12</sup>, Imperial College London, UK

### SUPPLEMENTAL MATERIAL

#### Detailed Methods

**Generation of transgenic mice.** A vector containing the  $\alpha$ MHC promoter<sup>1</sup> was modified to contain a versatile multiple cloning site ( $\alpha$ MHC-MCS); cDNA encoding for VSFP2.3<sup>2</sup> was inserted via NheI and HindIII to generate the  $\alpha$ MHC-VSFP2.3 plasmid (**Online Figure I**); sequence integrity was confirmed by restriction enzyme digestion and sequencing. For generation of transgenic mice, the  $\alpha$ MHC-VSFP2.3 fragment (7,783 bp; **Figure 1A**) was released by BamHI/PmeI digestion and microinjected into pronuclei of fertilized mouse oocytes (BDF1).  $\alpha$ MHC-GCaMP<sup>3</sup> mice were generated as reporter controls with known cardiac toxicity using a similar strategy.

**Echocardiography.** Myocardial structure and function were assessed by echocardiography using a Vevo 2100 system (Visual Sonics Inc., Toronto, Canada) with a 18-38 MHz transducer (MS400). 15-16-week old mice were anaesthetized with 1.5% isoflurane in 1.5 l/min 5% CO<sub>2</sub>/95% O<sub>2</sub> through a nozzle while heart rate and electrocardiogram (ECG) were monitored and recorded. Throughout the procedure, temperature was recorded with a rectal probe and maintained at 37°C with a heat pad and infrared light.

**Isolation of adult mouse cardiac myocytes.** Cardiomyocytes were isolated from adult transgenic mice according to a published protocol with modifications<sup>4, 5</sup>. In brief, hearts were quickly excised after cervical dislocation and Langendorff-perfused with modified Tyrode's solution containing (in mmol/L): NaCl 120, KCl 4.7, KH<sub>2</sub>PO<sub>4</sub> 0.6, Na<sub>2</sub>HPO<sub>4</sub> 0.6, MgSO<sub>4</sub> 1.2, Na-HEPES 10, NaHCO<sub>3</sub> 4.6, Taurine 30, 2,3-butanedione monoxime (BDM) 10, and Glucose 5.5 at the rate of 3-4 ml/minute at 37°C via the aorta. After 5 minutes, the perfusion was switched to buffer containing 400 U/mL collagenase type II (Worthington, Lakewood, NJ) and 12.5  $\mu$ mol/L CaCl<sub>2</sub> until the hearts became pale and swollen. Subsequently, ventricles were cut into small pieces with fine scissors. Cardiomyocytes were further dissociated by gentle trituration and purified by passing through a 200  $\mu$ m cell strainer. Finally, calcium concentration was increased stepwise to 1.2 mmol/L. Quiescent cells with rod-shaped morphology were used for further experiments.

**Immunofluorescence staining.** Isolated adult cardiomyocytes were adhered to laminin-coated coverslips, washed with PBS, and fixed with 4% formaldehyde (Histofix). Cells were permeabilized and blocked in

1% BSA/0.5% Triton X-100 for 2 hours at room temperature and subsequently incubated with mouse anti-RyR2 (1:500; Thermo Scientific, MA3-925) and anti-Ca<sub>v</sub>1.2 (1:500; Alomone labs, ACC-003) antibodies for 90 min at room temperature. After washing with blocking buffer three times for 5 min, cells were incubated with suitable secondary antibodies (**Online Table I**) for 1 h at room temperature, washed again three times for 5 min with blocking buffer and then PBS for 5 min before mounting with Fluoromount-G (SouthernBiotech) on glass slides. Localization of CFP and YFP as well as RyR2 and Ca<sub>v</sub>1.2 was examined by confocal laser scanning microscopy (LSM710/NLO, Zeiss).

**RNA-sequencing (RNA-seq) and bioinformatics.** Total RNA was isolated from the left ventricular free walls of 2 wild-type and 2 VSFP2.3#123 transgenic mice of different age (19 and 35 weeks; two independent litters from the same parents: ♂ - #434 [VSFP2.3#123] x ♀ - #379 [WT]; siblings were sex matched) using standard protocols (NucleoSpin RNA kit, Macherey-Nagel). RNA integrity was assessed with the Agilent Bioanalyzer 2100: RNA integrity number (RIN) was > 7 for all samples. RNA was subjected to library preparation (TruSeq Stranded Total RNA Sample Prep Kit, Illumina) and RNA-seq on an Illumina HighSeq-2000 platform (SR 50 bp; >40 Mio reads/sample). The raw RNA-seq reads (FASTQ) were mapped to mm10 using STAR<sup>6</sup> and analyzed using DESeq2<sup>7</sup>. Genes with an average RPKM<sup>8</sup>-value of >1 were considered expressed and identified as differentially regulated using a minimum absolute log<sub>2</sub> fold change of 1 and Benjamin & Hochberg adjusted p-value (FDR) of 0.05. VSFP2.3 transcript abundance was estimated by aligning raw FASTQ RNA reads to the VSFP CDS clone sequence using bowtie2. Gene ontology (GO) enrichment analysis of bioprocesses was performed with GOSep<sup>9</sup>. RNA-seq data was deposited in the NCBI's Gene Expression Omnibus (GEO series accession number GSE69190).

**Combined patch-clamp and fluorescence recordings in adult cardiomyocytes.** To determine the voltage-fluorescence relationship, a setup combining patch clamp with fluorescent imaging was established (**Online Figure II**). Isolated adult cardiomyocytes were placed in a custom made recording chamber mounted on an inverted microscope (Nikon TE-2000) equipped with a 40x/1.3 NA oil immersion objective and superfused with modified Tyrode's solution (in mmol/L: NaCl 130, KCl 4, NaHCO<sub>3</sub> 18, MgCl<sub>2</sub> 1.2, CaCl<sub>2</sub> 1.8, HEPES 10, glucose 10; pH 7.4 adjusted with NaOH; 37°C). Experiments were performed using the patch-clamp technique under whole-cell configuration using Axopatch 200B (Molecular Devices) or HEKA EPC 10 USB (HEKA) amplifiers. Patch pipettes were filled with a solution consisting of (in mmol/L): potassium gluconate 125, KCl 10, HEPES 5, EGTA 5, MgCl<sub>2</sub> 2, CaCl<sub>2</sub> 0.6, Na<sub>2</sub>ATP 4, pH 7.2/KOH. Cells were illuminated by a computer-controlled monochromator (Optoscan, Cairn Research). Excitation light (437/20 nm) was provided to the objective via a dichroic mirror (458 nm). Emitted light was first split by a 514 nm dichroic mirror. The reflected light (<514 nm) was filtered by a cyan emission filter (483/32 nm BP). The transmitted light (>514 nm) was then separated by a third dichroic (600 nm). The reflected light (<600 nm) was filtered by a yellow emission filter (514 nm LP). Cyan and yellow light was detected with two photomultiplier tubes connected to the Optoscan system. Light with wavelength longer than 600 nm (NIR) was imaged using a camera for observation of the cell during experiment.

Voltage-dependent fluorescence changes were assessed in voltage-clamp mode. Membrane potential of the cardiomyocytes was clamped at a holding potential of -70 mV, followed by 100 ms voltage steps ranging from -100 mV to +50 mV with 10 mV increments. Cyan and yellow fluorescence were recorded simultaneously. For each voltage step the ratio of yellow to cyan fluorescence intensity was calculated and normalized to the baseline ratio before the test pulse ( $R_0$ ). The change in baseline normalized ratio ( $\Delta R/R_0$ ) at the end of each test pulse was plotted against test pulse voltage and fitted using a Boltzmann equation to determine the full dynamic range of the voltage sensor and its half-maximal response ( $V_{1/2}$ ). Kinetics of sensor activation and deactivation were determined by fitting the fluorescence ratio traces with single or double exponential functions using Fitmaster (HEKA). Time constants were plotted versus test pulse voltage to assess voltage dependence of activation and deactivation of the sensor. In current-clamp experiments, APs were triggered by injecting 2 nA/2 ms

currents at 1 Hz. Fluorescence signals were analyzed by calculating  $\Delta R/R_0$  as above, low pass filtered (cutoff 500 Hz), and then analyzed along with the electrical APs to determine APD values. The Pearson's correlation coefficient was calculated between APD values obtained by patch-clamp and FRET recordings. Finally, pre-recorded APs of human embryonic stem cell (hESC) cardiomyocytes and human left ventricular cardiomyocytes were imposed on VSFP2.3 expressing mouse cardiomyocytes in voltage-clamp mode to assess VSFP2.3 responses to longer, simulated human APs.

**Whole heart optical mapping.** Adult mice (backcrossed into CD-1 background for >5 generations) of either sex with an age between 12 and 16 weeks were sacrificed by cervical dislocation under isoflurane anesthesia. The hearts were cannulated through the aorta with a blunt 21G needle, and mounted on a Langendorff-setup and gravity perfused with Tyrode's solution (mmol/L): NaCl 130, NaHCO<sub>3</sub> 24, KCl 4, MgCl<sub>2</sub> 1, CaCl<sub>2</sub> 1.8, KH<sub>2</sub>PO<sub>4</sub> 1.2, and D-glucose 5.6 supplemented with 1% bovine serum albumin (Sigma) and insulin (5 IU/L, Insuman Rapid, Sanofi-Aventis) equilibrated with carbogen (95% O<sub>2</sub>, 5% CO<sub>2</sub>) at 37°C. Blebbistatin (5 μmol/L; Sigma) was added to suppress motion artifacts unless otherwise indicated. After 10 min equilibration, the hearts were paced from the anterior free wall with 2 ms current (2.5 mA) pulses, using a bipolar point electrode (50-100 kΩ, FHC, USA) at 10 Hz. Custom-made Ag-AgCl ECG electrodes placed horizontally and parallel to the main heart axis at the epicardial surface were used for volumetric ECG recordings. Hearts were imaged (MVPLAPO 0.63x, NA0.15, Olympus) at 4x under 100 W short-arc mercury lamp (HBO103W/2, Olympus, Germany) illumination, using a 438±24 nm BP filter (CFP excitation, Semrock) and a dichroic mirror (480 nm). Emitted light was band passed by a 542±27 nm filter (YFP emission, Semrock, Inc) and recorded with a 100x100 pixel CMOS camera (Ultima-L, SciMedia USA Ltd.) at a frame rate of 500 Hz. Recordings were performed during spontaneous sinus rhythm or electrode pacing as indicated. The data were acquired and analyzed by custom-made software programmed in Java and Matlab (Mathworks).

**Fiber optic recordings.** To explore the possibility for minimally invasive recordings of VSFP2.3 signals, we constructed a dedicated fiber optic set-up. Briefly, three polymethyl methacrylate (PMMA) fibers (1 mm individual fiber diameter, Edmund Optics Inc) were assembled into a triangular array. Illumination provided by a metal halide lamp (Photofluor II, 200W, AHF analysentechnik AG) passed a filter cube (excitation filter: ET436±20 nm; excitation dichroic: 455 nm LF) and was guided through the optic fiber bundle to directly illuminate the heart. The emission light was collected by the same fiber bundle, passed through a second (emission) filter cube (emission dichroic: 510 nm LPXR, CFP: ET 480±40 nm, YFP: ET 535±30 nm), and directed to two EMCCD cameras (Cascade 128+, Photometrics) for separate recordings of CFP and YFP signals. Proof-of-concept experiments were performed first in Langendorff-perfused hearts and subsequently in anesthetized (2% isoflurane) and mechanically ventilated mice via a left lateral thoracotomy.

**Generation of αMHC-VSFP2.3/neoR induced pluripotent stem cell lines.** iPSCs were generated from tail tip fibroblasts (TTFs) of a double transgenic mouse expressing VSFP2.3 and a neomycin resistance gene (NeoR) under the control of the cardiomyocyte restricted αMHC promoter (**Online Figure IIIA**) according to standard protocols. Passage 2 TTFs were subjected to reprogramming with the STEMCCA (OKSM) lentiviral reprogramming system<sup>10</sup>. Stem cell colonies were isolated and cultured according to standard protocols. The genotype was confirmed by PCR and evidence for pluripotency was collected by RT-PCR and immunofluorescent staining for stemness markers (Oct3/4, Nanog, Rex1, Sox 2 and SSEA1; **Online Table I**).

**Differentiation and selection of cardiomyocytes from αMHC-VSFP2.3/neoR iPSCs.** Cardiac differentiation was performed in spinner flasks for 11 days in Iscove's medium supplemented with 20% fetal calf serum, 1% non-essential amino acids, 100 U/L penicillin, 100 μg/mL streptomycin, 2 mmol/L L-glutamine, 240 μmol/L L-ascorbic acid, and 100 μmol/L β-mercaptoethanol followed by additional 7 days of G418 (200 μg/mL) for cardiomyocyte selection. Resulting embryoid bodies (EBs) showed

spontaneous beating and were subsequently dissociated by incubation in collagenase I at 37°C for 1 h into single cardiomyocytes. Purity of cardiomyocytes was assessed by flow cytometry (BD LSR III) after staining for sarcomeric  $\alpha$ -actinin (Sigma). iPSC-derived cardiomyocytes were cultured as monolayers in above mentioned Iscove's medium for additional 5 or 12 days. CFP and YFP were detected in living cells by a laser scanning confocal microscopy (LSM710/NLO, Zeiss). For FRET imaging, iPSC-derived cardiomyocytes were plated on custom-made recording chambers, paced at 1 Hz under field stimulation, and recorded with a dual photomultiplier (PMTs) setup (IonOptix) with appropriate CFP and YFP filters (CFP excitation: 436±20 nm; emission ET 480±40 nm [CFP] and 535±30 nm [YFP]).

### **Online Figure, Table, and Video Legends**

**Online Figure I. Schematic of the cloning strategy.** **A.** Vector containing the cardiac specific alpha myosin heavy chain ( $\alpha$ MHC) promoter sequence and a unique multiple cloning site (MCS). **B.** cDNA encoding for VSFP2.3 was released with NheI and HindIII and inserted into the  $\alpha$ MHC-MCS vector. **C.** The resulting vector with VSFP2.3 under the control of the  $\alpha$ MHC promoter ( $\alpha$ MHC-VSFP2.3); DNA sequence for pronucleus injection was released by BamHI/Pme I double digestion.

### **Online Figure II. Setup for simultaneously recording of electrical APs and optical APs.**

**Online Figure III. Generation of  $\alpha$ MHC-VSFP2.3/neoR iPSC-lines.** **A.** Double transgenic mice ( $\alpha$ MHC-VSFP2.3/neoR) were bred according to the depicted mating strategy. **B.** Tail tip fibroblasts (TTF; left photograph; Scale bar: 200  $\mu$ m) from a  $\alpha$ MHC-VSFP2.3/neoR mouse were subjected to OSKM reprogramming to yield iPSC colonies (right photograph; Scale bar: 200  $\mu$ m; inset: 50  $\mu$ m). Expression of pluripotency markers was confirmed in 6 iPSC-clones by RT-PCR; expression was compared to transcript levels in embryonic stem cells (ESC-A6-line) and TTF (bottom panel). **C.** Immunofluorescent staining of  $\alpha$ MHC-VSFP2.3/neoR iPSC for the indicated pluripotency markers. Scale bars: 50  $\mu$ m.

**Online Figure IV. Summary of echocardiography data.** **A.** Echocardiography data from wild-type (WT) and VSFP2.3 transgenic mouse lines (refer also to **Fig. 2A-D**). **B-E.** Additional echocardiography data from aging cohorts of WT and VSFP2.3#123 mice. Note that each mouse was subjected to echocardiography twice within a time-frame of 3 weeks. White and black bars represent the 16 week data in WT and VSFP2.3#123 mice. Blue and red trajectories denote data from aging (21-32 weeks of age) WT and VSFP2.3#123 mice, respectively.

**Online Figure V. Enhanced VSFP-signal decay under isoprenaline and electrical pacing.** Cardiomyocytes isolated from adult VSFP2.3 transgenic mice were subjected to optical imaging (IonOptix) at room temperature to assess action potential duration (APD) under adrenergic stimulation with isoprenaline (1  $\mu$ mol/L, n=6 cardiomyocytes; **A**) and increasing electrical field stimulation (0.5-2 Hz, n=4 cardiomyocytes; **B**). \*p < 0.05 vs. baseline by student's t-test (**A**) and one-way ANOVA with Tukey multiple comparisons test (**B**).

**Online Figure VI. Simultaneous recordings of electrical and optical APs in iPSC-derived cardiomyocytes.** **A.** Simultaneous patch-clamp (top) and optical (bottom) recordings of an AP in an iPSC-derived cardiomyocyte at room temperature. Depicted is the average of 10 APs with SEM. **B.** Linear correlation with confidence interval between optical APD<sub>50</sub> and electrical APD<sub>90</sub> (22 individual APs from 2 cardiomyocytes analyzed).

**Online Table I. List of primers and antibodies used in the study.**

**Online Table II. Electrophysiological properties of cardiomyocytes isolated from adult wild-type (WT) and VSFP2.3 (line #123) mice.** RMP: resting membrane potential; Overshoot: maximal positive potential; APA: AP amplitude;  $dV/dt_{max}$ : maximal upstroke velocity;  $APD_{90}$ : AP duration at 90% of repolarisation. p-Values by unpaired two-sided student's t-test.

**Video File I: spread of excitation during sinus rhythm.** A screen shot is provided in Figure 5A.

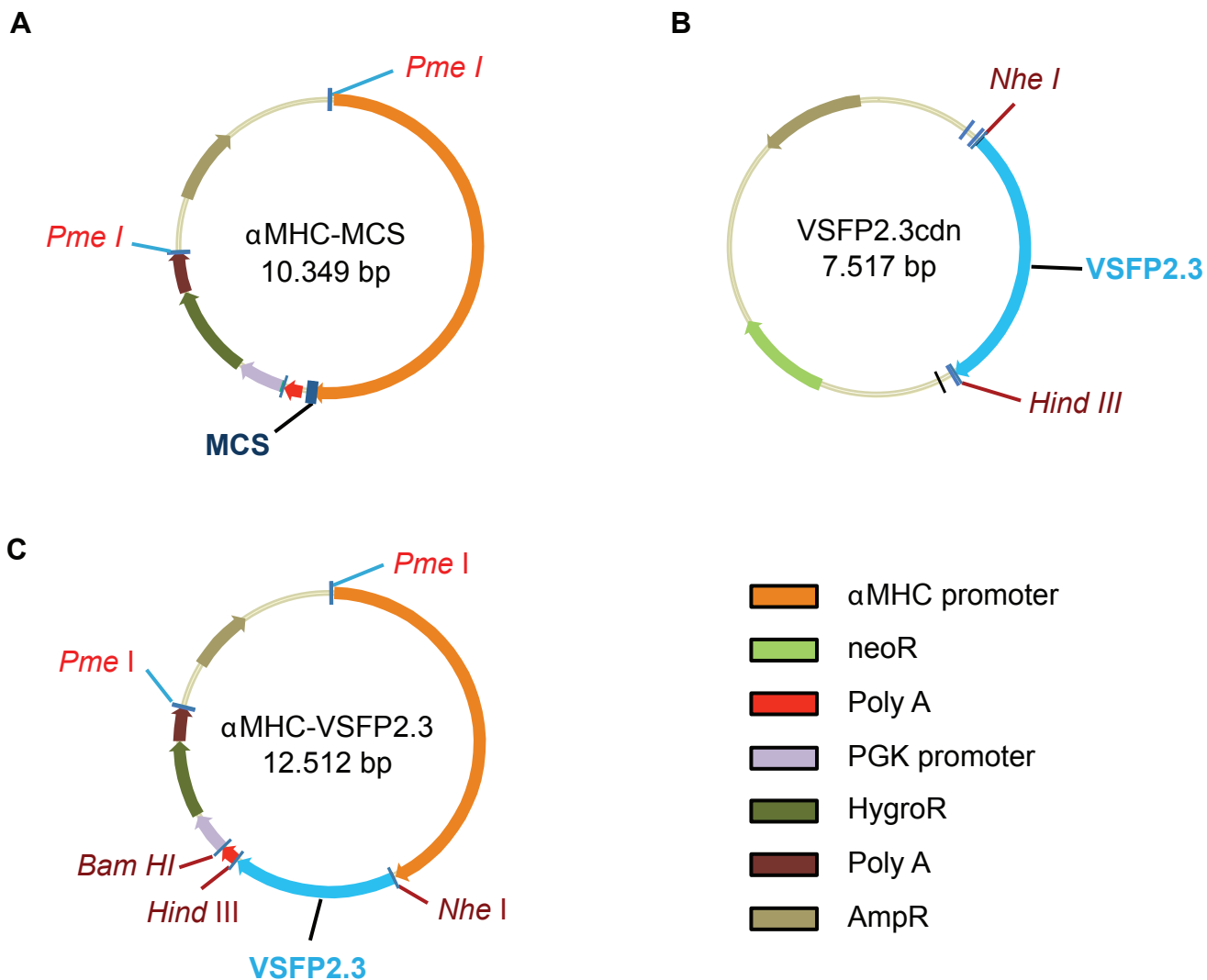
**Video File II: spread of excitation during 10 Hz pacing.** Screen shots are provided in Figure 5B.

**Video File III: imaging of a ventricular arrhythmia.** The recording was after termination of the 12.5 Hz 200-pulse train for arrhythmia induction. Screen shots are provided in Figure 5B.

### Supplemental References

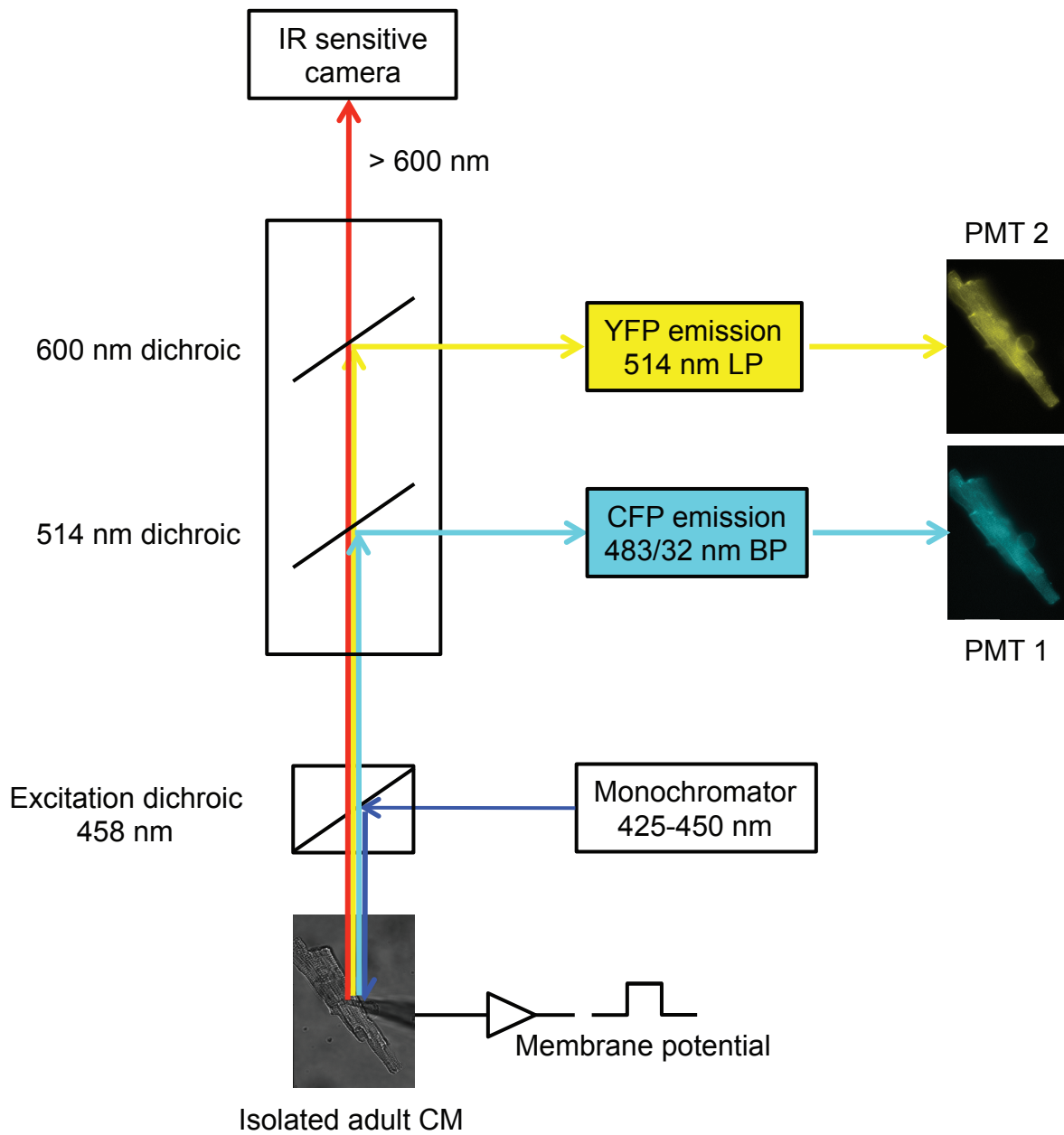
1. Subramaniam A, Jones WK, Gulick J, Wert S, Neumann J, Robbins J. Tissue-specific regulation of the alpha-myosin heavy chain gene promoter in transgenic mice. *The Journal of biological chemistry*. 1991;266:24613-24620
2. Lundby A, Mutoh H, Dimitrov D, Akemann W, KnOpfel T. Engineering of a genetically encodable fluorescent voltage sensor exploiting fast ci-vsp voltage-sensing movements. *PLoS ONE*. 2008;3:e2514
3. Tallini YN, Ohkura M, Choi BR, Ji G, Imoto K, Doran R, Lee J, Plan P, Wilson J, Xin HB, Sanbe A, Gulick J, Mathai J, Robbins J, Salama G, Nakai J, Kotlikoff MI. Imaging cellular signals in the heart in vivo: Cardiac expression of the high-signal  $ca^{2+}$  indicator gcamp2. *Proceedings of the National Academy of Sciences of the United States of America*. 2006;103:4753-4758
4. Kabaeva Z, Zhao M, Michele DE. Blebbistatin extends culture life of adult mouse cardiac myocytes and allows efficient and stable transgene expression. *American journal of physiology. Heart and circulatory physiology*. 2008;294:H1667-1674
5. O'Connell TD, Rodrigo MC, Simpson PC. Isolation and culture of adult mouse cardiac myocytes. *Methods Mol Biol*. 2007;357:271-296
6. Dobin A, Davis CA, Schlesinger F, Drenkow J, Zaleski C, Jha S, Batut P, Chaisson M, Gingeras TR. Star: Ultrafast universal rna-seq aligner. *Bioinformatics*. 2013;29:15-21
7. Love MI, Huber W, Anders S. Moderated estimation of fold change and dispersion for rna-seq data with deseq2. *Genome biology*. 2014;15:550
8. Mortazavi A, Williams BA, McCue K, Schaeffer L, Wold B. Mapping and quantifying mammalian transcriptomes by rna-seq. *Nature methods*. 2008;5:621-628
9. Young MD, Wakefield MJ, Smyth GK, Oshlack A. Gene ontology analysis for rna-seq: Accounting for selection bias. *Genome biology*. 2010;11:R14
10. Somers A, Jean JC, Sommer CA, Omari A, Ford CC, Mills JA, Ying L, Sommer AG, Jean JM, Smith BW, Lafyatis R, Demierre MF, Weiss DJ, French DL, Gadue P, Murphy GJ, Mostoslavsky G, Kotton DN. Generation of transgene-free lung disease-specific human induced pluripotent stem cells using a single excisable lentiviral stem cell cassette. *Stem Cells*. 2010;28:1728-1740

## Online Figure I



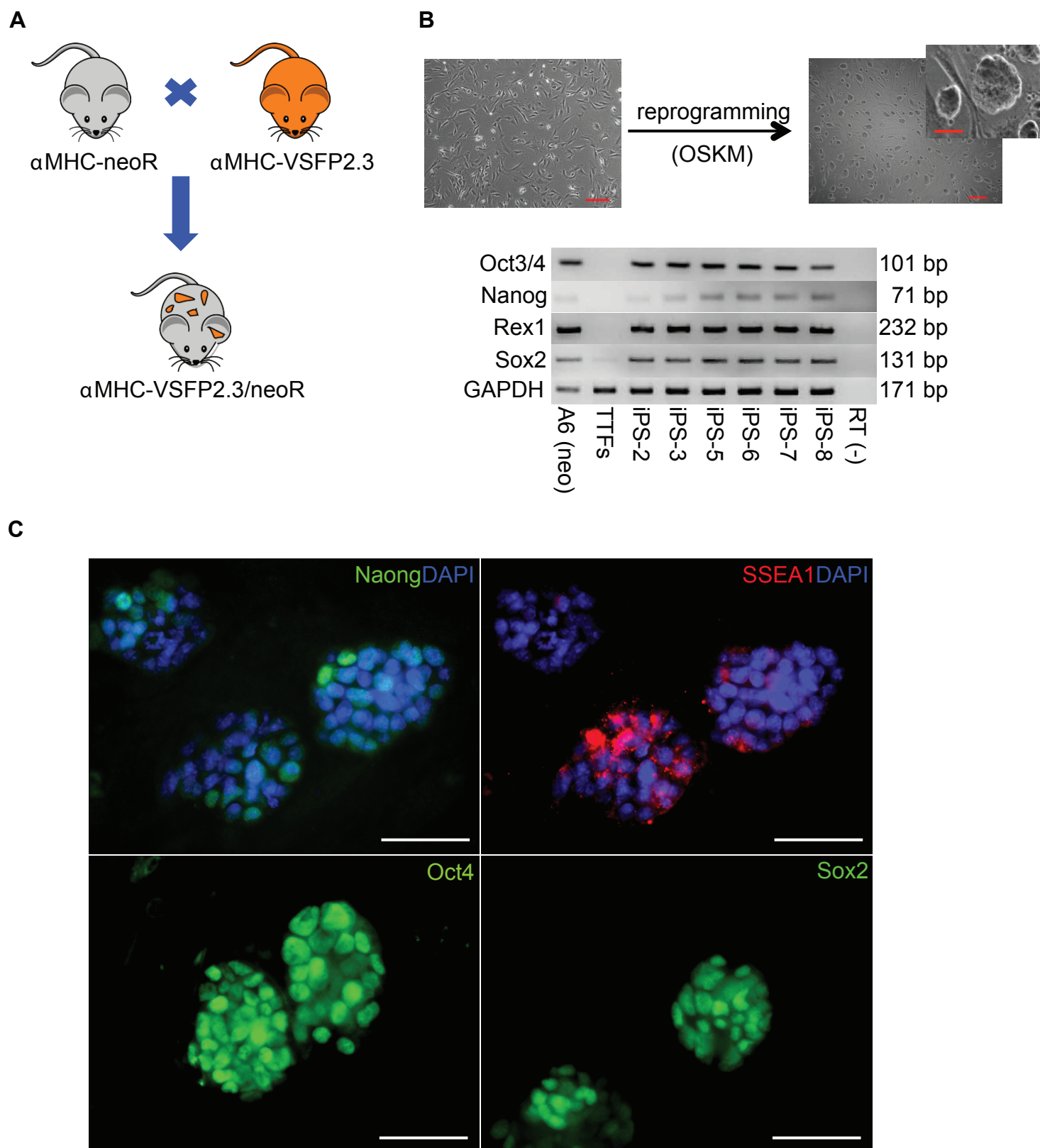
**Online Figure I. Schematic of the cloning strategy.** **A.** Vector containing the cardiac specific alpha myosin heavy chain ( $\alpha$ MHC) promoter sequence and a unique multiple cloning site (MCS). **B.** cDNA encoding for VSFP2.3 was released with *Nhe*I and *Hind*III and inserted into the  $\alpha$ MHC-MCS vector. **C.** The resulting vector with VSFP2.3 under the control of the  $\alpha$ MHC promoter ( $\alpha$ MHC-VSFP2.3); DNA sequence for pronucleus injection was released by *Bam*HI/*Pme*I double digestion.

## Online Figure II



Online Figure II. Setup for simultaneously recording of electrical APs and optical APs.

### Online Figure III

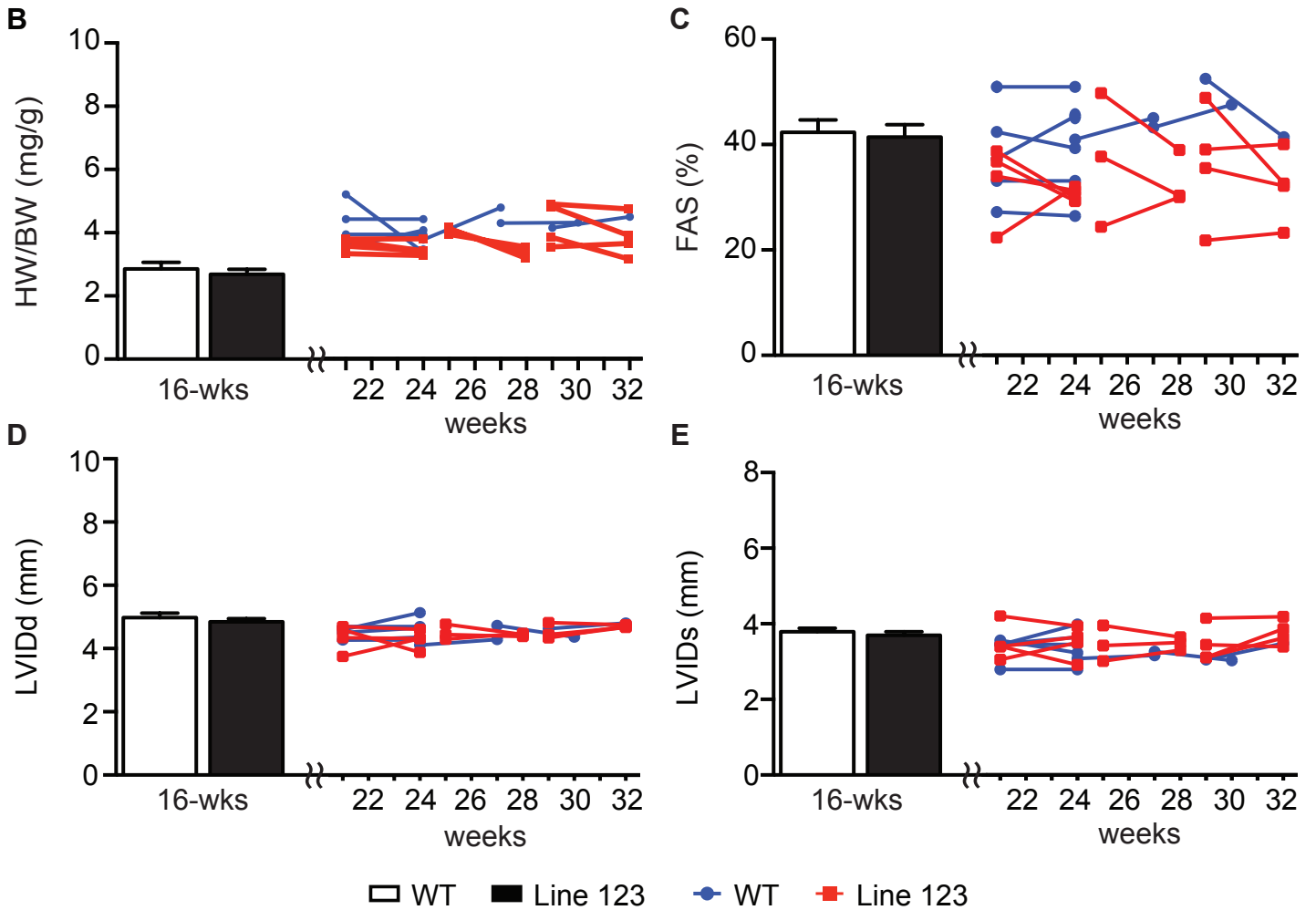


**Online Figure III. Generation of αMHC-VSFP2.3/neoR iPSC-lines.** **A.** Double transgenic mice (αMHC-VSFP2.3/neoR) were bred according to the depicted mating strategy. **B.** Tail tip fibroblasts (TTF; left photograph; Scale bar: 200 μm) from a αMHC-VSFP2.3/neoR mouse were subjected to OSKM reprogramming to yield iPSC colonies (right photograph; scale bars: 200 μm [inset: 50 μm]). Expression of pluripotency markers was confirmed in 6 iPSC-clones by RT-PCR; expression was compared to transcript levels in embryonic stem cells (ESC-A6-line) and TTF (bottom panel). **C.** Immunofluorescent staining of αMHC-VSFP2.3/neoR iPSC for the indicated pluripotency markers. Scale bars: 50 μm.

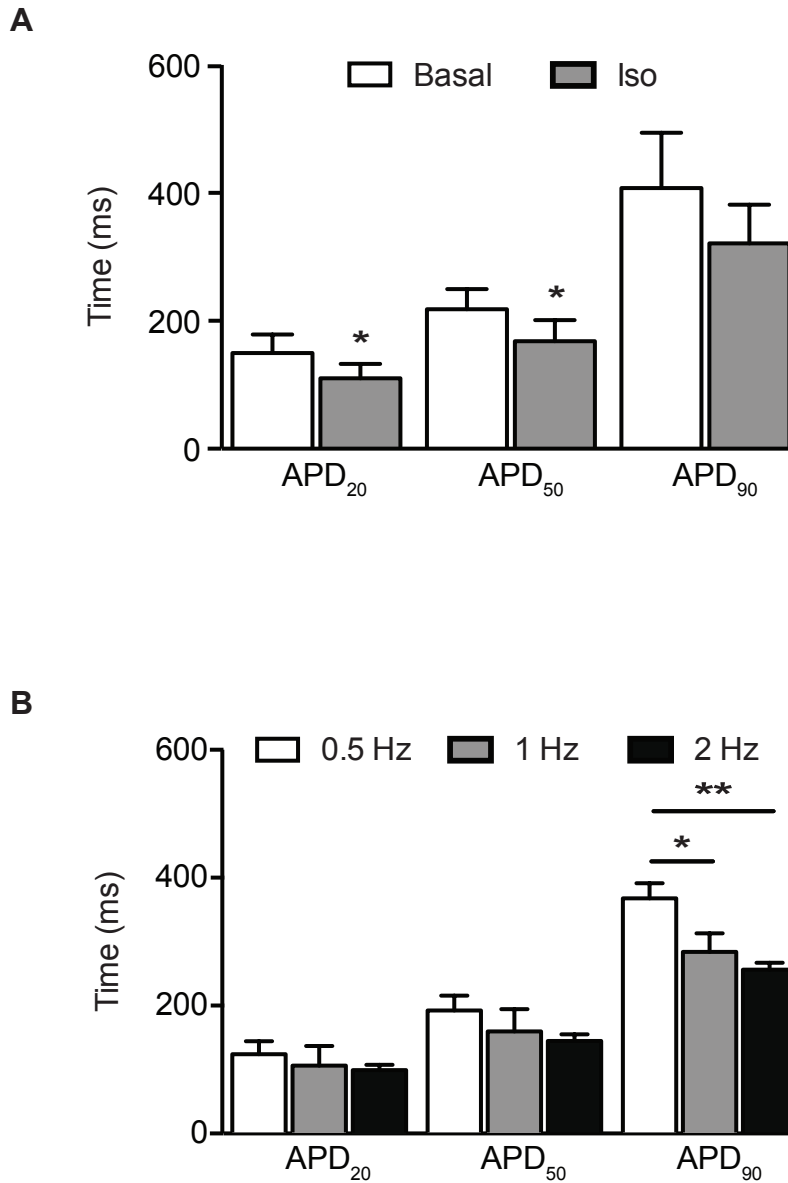
## Online Figure IV

**A**

	WT	Line 97	Line 107	Line 108	Line 123	GCaMP2
HR (bpm)	521±15	549±11	528±22	514±14	540±22	581±17
HW/BW (mg/g)	2.9±0.7	2.7±0.2	2.7±0.2	3±0.1	2.7±0.2	6.8±1.2
FAS (%)	42±2	39±3	42±5	45±3	41±2	5.6±1.8
CO (ml/min)	31±3	28±2	31±3	32±2	30±2	16±7
LVIDd (mm)	5.0±0.1	4.8±0.1	5.0±0.2	5.0±0.1	4.8±0.1	7.3±0.5
LVIDs (mm)	3.8±0.1	3.7±0.1	3.7±0.2	3.7±0.2	3.7±0.1	7.2±0.4
AWThF (%)	20±3	22±2	24±4	27±3	22±3	6.7±1.8
PWThF (%)	23±2	26±4	19±2	26±4	21±4	1.7±1

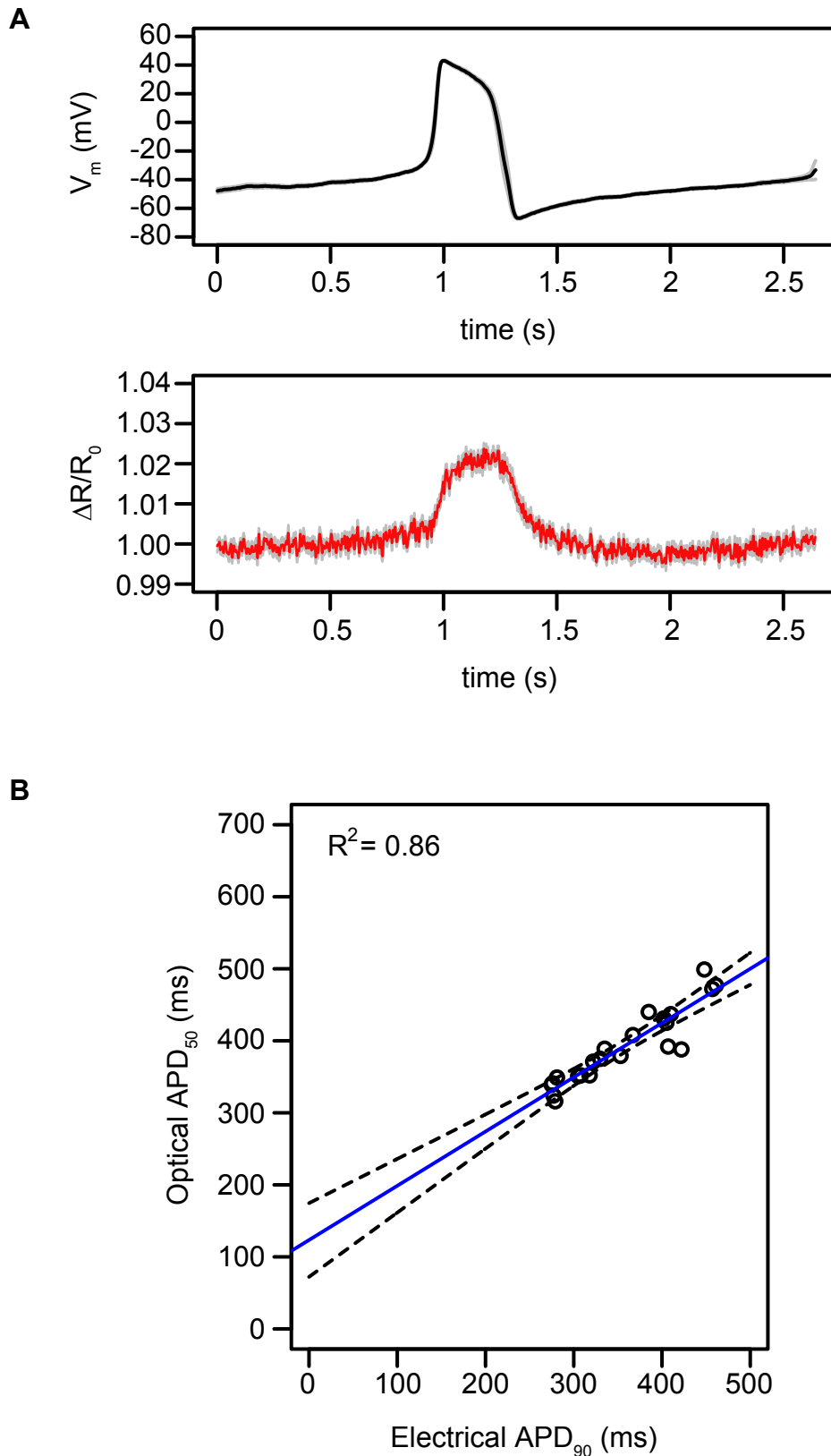


**Online Figure IV. Summary of echocardiography data.** **A.** Echocardiography data from wild-type (WT) and VSFP2.3 transgenic mouse lines (refer also to **Fig. 2A-D**). **B-E.** Additional echocardiography data from aging cohorts of WT and VSFP2.3#123 mice. Note that each mouse was subjected to echocardiography twice within a time-frame of 3 weeks. White and black bars represent the 16 week data in WT and VSFP2.3#123 mice. Blue and red trajectories denote data from aging (21-32 weeks of age) WT and VSFP2.3#123 mice, respectively.



**Online Figure V. Enhanced VSFP-signal decay under isoprenaline and electrical pacing.** Cardiomyocytes isolated from adult VSFP2.3 transgenic mice were subjected to optical imaging (IonOptix) at room temperature to assess action potential duration (APD) under adrenergic stimulation with isoprenaline (1  $\mu\text{mol/L}$ ,  $n=6$  cardiomyocytes; **A**) and increasing electrical field stimulation (0.5-2 Hz,  $n=4$  cardiomyocytes; **B**). \* $p < 0.05$  vs. baseline by student's t-test (**A**) and one-way ANOVA with Tukey multiple comparisons test (**B**).

## Online Figure VI



**Online Figure VI. Simultaneous recordings of electrical and optical APs in iPSC-derived cardiomyocytes.** **A.** Simultaneous patch-clamp (top) and optical (bottom) recordings of an AP in an iPSC-derived cardiomyocyte at room temperature. Depicted is the average of 10 APs with SEM. **B.** Linear correlation with confidence interval between optical APD<sub>50</sub> and electrical APD<sub>90</sub> (22 individual APs from 2 cardiomyocytes analyzed).

**Online Table I**

Gene	Sequences	Tm (°C)	Product size (bp)
Oct 3/4	Forward: 5'-GCCCCAATGCCGTGAAG- 3'	58	101 bp
	Reverse: 5'-CAGCAGCTTGGCAAACCTGTTC- 3'	60	
Nanog	Forward: 5'-TGCTACTGAGATGCTCTGCACA- 3'	60	71 bp
	Reverse: 5'-TGCCTTGAAGAGGCAGGTCT- 3'	59	
Sox2	Forward: 5'-GGCAGCTACAGCATGATGCAGGAGC- 3'	60	131 bp
	Reverse: 5'-CCTGCAGTACAACTCCATGACCAG- 3'	60	
Rex1	Forward: 5'-GGCCAGTCCAGAATACCAGA- 3'	59	232 bp
	Reverse: 5'- GAACTCGCTTCCAGAACCTG - 3'	59	
GAPDH*	Forward: 5'-ATGTTCCAGTATGACTCCACTCACG- 3'	63	171 bp
	Reverse: 5'- TGTCGTGGAGTCTACTGGTGTCTTC -3'	65	

\* Housekeeping gene

1 <sup>st</sup> Antibody				2 <sup>nd</sup> Antibody		
		Dilution	Supplier		Dilution	Supplier
RyR2	Mouse monoclonal	1:500	Thermo Scientific (MA3-916)	Alexa 568 goat anti-mouse	1:1000	Life Technologies
Cav1.2	Rabbit polyclonal	1:500	Alomone labs (ACC-003)	Alexa 633 goat anti-rabbit	1:1000	Life Technologies
Oct 4	Rabbit polyclonal	1:500	Abcam (ab19857)	Anti-rabbit IgG Alexa 488	1:800	Molecular Probes
Nanog	Rabbit polyclonal	1:500	Abcam (ab80892)	Anti-rabbit IgG Alexa 488	1:800	Molecular Probes
Sox2	Rabbit polyclonal	1:500	Abcam (ab97959)	Anti-rabbit IgG Alexa 488	1:800	Molecular Probes
SSEA1	Mouse monoclonal	1:50	Abcam (ab16285)	Anti-mouse IgG Alexa 546	1:800	Molecular Probes

**Online Table I. List of primers and antibodies used in the study.**

**Online Table II**

	RMP (mV)	Overshoot (mV)	APA (mV)	dV/dt <sub>max</sub> (V/s)	APD <sub>90</sub> (ms)
WT (n=7)	-79 ± 2	33 ± 4	111 ± 3	283 ± 14	53 ± 6
VSFP2.3 (n=7)	-79 ± 8	34 ± 4	113 ± 7	309 ± 16	55 ± 6
p-Value	0.92	0.88	0.87	0.23	0.81

**Online Table II. Electrophysiological properties of cardiomyocytes isolated from adult wild-type (WT) and VSFP2.3 (line #123) mice.** RMP: resting membrane potential; Overshoot: maximal positive potential; APA: AP amplitude; dV/dt<sub>max</sub>: maximal upstroke velocity; APD<sub>90</sub>: AP duration at 90% repolarization. p-Values by unpaired two-sided student's t-test.

## Sensing Cardiac Electrical Activity With a Cardiac Myocyte–Targeted Optogenetic Voltage Indicator

Mei-Ling Chang Liao, Teun P. de Boer, Hiroki Mutoh, Nour Raad, Claudia Richter, Eva Wagner, Bryan R. Downie, Bernhard Unsöld, Iqra Arooj, Katrin Streckfuss-Bömeke, Stephan Döker, Stefan Luther, Kaomei Guan, Stefan Wagner, Stephan E. Lehnart, Lars S. Maier, Walter Stühmer, Erich Wettwer, Toon van Veen, Michael M. Morlock, Thomas Knöpfel and Wolfram-Hubertus Zimmermann

*Circ Res.* 2015;117:401-412; originally published online June 15, 2015;  
doi: 10.1161/CIRCRESAHA.117.306143

*Circulation Research* is published by the American Heart Association, 7272 Greenville Avenue, Dallas, TX 75231  
Copyright © 2015 American Heart Association, Inc. All rights reserved.  
Print ISSN: 0009-7330. Online ISSN: 1524-4571

The online version of this article, along with updated information and services, is located on the World Wide Web at:

<http://circres.ahajournals.org/content/117/5/401>

Data Supplement (unedited) at:

<http://circres.ahajournals.org/content/suppl/2015/06/15/CIRCRESAHA.117.306143.DC1.html>

**Permissions:** Requests for permissions to reproduce figures, tables, or portions of articles originally published in *Circulation Research* can be obtained via RightsLink, a service of the Copyright Clearance Center, not the Editorial Office. Once the online version of the published article for which permission is being requested is located, click Request Permissions in the middle column of the Web page under Services. Further information about this process is available in the [Permissions and Rights Question and Answer](#) document.

**Reprints:** Information about reprints can be found online at:  
<http://www.lww.com/reprints>

**Subscriptions:** Information about subscribing to *Circulation Research* is online at:  
<http://circres.ahajournals.org/subscriptions/>